**The Iberia-Eurasia plate boundary east of the Pyrenees**

(Article begins on next page)

03 January 2025

**The Iberia-Eurasia plate boundary east of the Pyrenees**

Tavani S.[1], Bertok C.[2], Granado P.[3,4], Piana F.[5], Salas R.[4,6], Vigna B.[7], Muñoz J.A.[3,4]

1 - Dipartimento di Scienze della Terra, dell'Ambiente e delle Risorse, Università Federico II, Napoli, Italy.

2 - Dipartimento di Scienze della Terra, Università degli Studi di Torino, Torino, Italy

3 - Departament de Dinàmica de la Terra i de l'Oceà, Universitat de Barcelona, Barcelona, Spain

4 - Institut de Recerca Geomodels, Universitat de Barcelona, Barcelona, Spain

5 - CNR-IGG Torino, Italy

6 - Departament de Mineralogia, Petrologia i Geologia Aplicada, Universitat de Barcelona, Barcelona, Spain

7 - Dipartimento di Ingegneria dell'Ambiente, del Territorio e delle Infrastrutture, Politecnico di Torino, Torino, Italy

Corresponding Author: Stefano Tavani. stefano.tavani@unina.it

Highlights

The mid-Cretaceous Marguareis extensional system of the Western Alps is introduced

This system forms part of the eastern portion of the Iberia-Eurasia plate boundary

This eastern portion included structures of the SE France basin

The Early to mid-Cretaceous plate margin had a purely divergent movement

**Abstract**

In this work we provide a reappraisal of the mid-Cretaceous extensional basins located to the east of the Pyrenean mountain ranges, from the easternmost portion of Iberia to the Briançonnais Domain of the Western Alps fold-and-thrust belt. These features are reviewed and compared with those of the Bay of Biscay-Pyrenean rift, with the aim of defining geometry, kinematics, timing and lateral extent of the eastern termination of the Mesozoic Iberia-Eurasia plate boundary. Timing and direction of extension, as well as the style of structural segmentation in the Bay of Biscay - Pyrenean rift, are similar to those of basins exposed to the east of the Pyrenean mountain ranges. In both areas, the divergent movement between Iberia and Eurasia caused NNE-SSW oriented extension recorded in WNW-ESE elongated Late Jurassic to mid-Cretaceous basins, segmented by NNE-SSW trending transfer zones.

In this work we also individuate and introduce the eastern termination of the Iberia-Eurasia plate boundary. This is the Marguareis extensional system of the Briançonnais Domain of the SW Alps. The crustal-scale Marguareis extensional system involves Paleozoic and Mesozoic rocks and includes a tens of km long transfer fault flanking an extensional domino array that accounted for ca. 2 km of extension along 6 km long sections. When post-Cretaceous alpine rotation is removed, the mid-Cretaceous transfer fault and the extension direction of the Marguareis extensional system become oriented parallel to those of the other portions of the plate boundary, indicating its pertinence to the Bay of Biscay-Pyrenean rift system.

Reviewed and newly presented data about the mid-Cretaceous tectonics spanning from the easternmost portion of Iberia to the Western Alps indicate that: (i) the Marguareis extensional system and the extensional structures of south France constituted the easternmost portion of the segmented and laterally terminating Bay of Biscay-Pyrenean rift system; (ii) this easternmost portion of the Iberia-Eurasia plate boundary was characterised by a purely divergent Early to mid-Cretaceous movement.

2

## 1 Introduction

### 1.1 The Cretaceous Iberia-Eurasia plate boundary controversy

The geometry, kinematics, and lateral extent of the Iberia-Eurasia plate boundary during the Cretaceous period remains a question of considerable debate among earth scientists. The origin of such debate goes back to the dawn of plate tectonics and underlies on the mechanism by which the Bay of Biscay opened. Indeed, during the early 70's, three main hypotheses about the opening of the Bay of Biscay were postulated (Choukroune et al., 1973). In this early work the opening of the V-shaped Bay of Biscay was described in terms of the rotation of Iberia around Eulerian poles that would have been approximately located either (i) to the east of Iberia (Fig. 1a), (ii) close to Paris (Fig. 1b), or (iii) within the Pyrenean mountain range (Fig. 1c). Each of these hypotheses has different implications for the opening mode of the Bay of Biscay and implies contrasting amounts of rotation for Iberia with respect to Eurasia: the first hypothesis entails a rift-perpendicular opening mode for the Bay of Biscay by means of an eastward diminishing divergence between Iberia and Eurasia. The second one involves a left-lateral motion of Iberia with respect to Eurasia along a dominant strike-slip transform plate boundary. The third hypothesis implies divergence between Iberia and Eurasia in the Bay of Biscay coeval with convergence between these two plates east of the Euler pole in the NE corner of Iberia (i.e., scissor-type model).

In the light of geological and geophysical research during the last 40 years, these early models have been updated and improved as shown by the works of Jammes et al. (2009) and Tugend et al. (2014) in regards of the rift-perpendicular opening mode (Fig. 1a); those of Olivet (1996) or Stampfli and Borel (2002) in relation to the strike-slip mode (Fig. 1b), or the scissor-type mode (Fig. 1c) by Sibuet et al. (2004), Vissers and Meijer (2012), and Vissers et al. (2016).

Despite the amount of data and scientific outputs, the debate is far from over. One of the main reason for this is provided by the uncertainties associated with the data constraining the Cretaceous movement of Iberia. As an example, while it is undisputed that Iberia underwent a certain amount of counter-clockwise rotation with respect to Europe coevally with the opening of

3

the Bay of Biscay (van der Voo, 1969), the published vertical axis rotation values span between 20° to 40° (see Neres et al., 2012 and Barnett-Moore et al., 2016 for recent reviews). It is also unclear whether the rotation took place during a large portion of the Cretaceous period (Galdeano et al., 1989), or was only limited to the Aptian stage (Gong et al., 2008; Vissers et al., 2016). Similarly, the nature and age of the Bay of Biscay floor have received different interpretations: many authors support the occurrence of a large domain of exhumed subcontinental mantle in the Bay of Biscay (e.g. Thinon et al., 2003; Jammes et al., 2009; Roca et al., 2011; Tugend et al., 2014; Manatschal et al., 2015; Nirrengarten et al., 2017), whereas other workers lean towards a largely oceanic nature (e.g. Sibuet et al., 2004; Vissers and Meijer, 2012) or a mixed model of intruded exhumed mantle (Pedreira et al., 2015). These different ideas about the nature of the Bay of Biscay imply different interpretations for the age and significance of some of the magnetic anomalies (Sibuet et al., 2004) and, ultimately, entail different positions for Iberia at the beginning of the Bay of Biscay opening. The reliability of geological data in constraining the plate tectonic evolution of this large domain has also been questioned. The absence of any evidence for a mid-Cretaceous convergence stage in the Pyrenean area is striking, as the Pyrenean area was experiencing a well-constrained extensional regime during that time (e.g. Muñoz, 2002; Vergés et al., 2002; Jammes et al., 2009). However, while many authors argue that this makes the scissor-type scenario unrealistic (e.g. Tugend et al., 2014), others frame the mid-Cretaceous extension within the development of back-arc basins associated with the subduction of oceanic crust (Sibuet et al., 2004). In summary, the scissor-type model has its strength in the interpreted pattern of magnetic anomalies, and in the predicted amount of vertical axis rotation of Iberia. However, it is not proved that all the interpreted magnetic anomalies in the Bay of Biscay floor correspond to a Penrose-type oceanic crust. In addition, there is no evidence for an ophiolitic sequence preserved in the Pyrenees, under the Ebro foreland basin or along the Catalan Coastal Ranges. The weakest argument for the scissor-type scenario is the lack of any unequivocal geological proof for mid-Cretaceous convergence in the NE Iberia. On the other hand, the strike-slip scenario is consistent with the amount of vertical axis rotation documented for

Iberia as well; it partly fits with the magnetic anomalies, but the geological evidence for hundreds of kilometres of left-lateral motion of Iberia during the mid-Cretaceous is missing. Therefore, the rift-perpendicular solution is the most geologically-supported scenario. It is also consistent with the pattern of magnetic anomalies for the area where no mantle exhumation is inferred. Its weakest point though is the amount of vertical axis rotation: the coeval opening of the Bay of Biscay and the Pyrenean arm requires, if the Iberian plate is considered rigid, a Euler pole to the east of Iberia, which implies values of rotation of nearly 10° (Choukroune et al., 1973), largely below the published ones (e.g. van der Voo, 1969). Another problem with the rift-perpendicular model is the expected left-lateral movement of Iberia as the Atlantic opening progressed northward of the Azores-Gibraltar transfer zone at Late Jurassic-Early Cretaceous times (Stampfli and Hochard, 2009). Ultimately, each of these three scenarios apparently has its strengths and weaknesses and none of them can fully reconcile the available geological and geophysical datasets.

The key observation to solve this problem is that each of the three postulated hypotheses implies a different style of termination for the eastern Iberia-Eurasia plate boundary (Fig. 2). In fact, an additional controversy arises when joining the opening of the Bay of Biscay-Pyrenean rift with the Alpine Tethys further east, in particular with the so-called Valais "ocean" (e.g. Stampfli et al., 1998; Stampfli and Hochard, 2009; Beltrando et al., 2012). In the rift perpendicular scenario, as proposed by Manatschal and Muntener (2009), the Bay of Biscay-Pyrenean rift and the Alpine Tethys are diachronous and non-connected rifts, as the former is thought to terminate eastwards around the NW continental margin of the Alpine Tethys (Fig. 2a). Coherently, the Sardinia-Corsica-Briançonnais block is considered part of both Iberia and Eurasia. In the strike-slip type scenarios, the left-lateral motion of Iberia with respect to Eurasia is partly or completely accommodated to the east by the development of the Valais "ocean" (Fig. 2b). This ocean is interpreted by several authors as a mid-Cretaceous branch of the Jurassic Alpine Tethys; it would represent a sort of dilation jog of the North Pyrenean Fault (e.g. Stampfli and Borel, 2002; Rosenbaum and Lister, 2005; Handy et al., 2010), establishing the connection between the Bay of Biscay-Pyrenean rift system and the

Alpine Tethys, and separating the Sardinia-Corsica-Briançonnais block from Eurasia. However, the nature and position of the Valais "ocean" within the nearby spreading systems is significantly biased by the complexity of the Alpine thrust stacking and folding and associated metamorphism (e.g., Schmid et al., 2004; Froitzheim et al., 2008). Importantly, the reported mid-Cretaceous spreading ages for the Valais "ocean" have been challenged by U-Pb dating of magmatic zircons which have provided disparate spreading ages, from Early Carboniferous (337 Ma; Bussy et al., 2008), to Permian (267 and 272 Ma; Beltrando et al., 2007), or even Late Jurassic (163-155 Ma; Liati and Froitzheim, 2006). In the scissor-type scenario, the Pyrenean arm is connected to the Alpine Tethys as well. However, the connection is not ensured by the Valais "ocean" but, rather, the Pyrenean arm is considered part of the Alpine Tethys undergoing north-ward subduction during the mid-Cretaceous. The occurrence of a transform zone bounding the subduction to the east is forecast (e.g. Advokaat et al., 2014), kinematically separating the Corsica-Sardinia-Briançonnais block from Iberia (Fig. 2c), which implies that this block was part of Eurasia.

The reconstruction of the Mesozoic palaeogeography immediately east of the Pyrenees, (Fig. 3) is not straightforward. This area has been strongly modified by the Cenozoic convergence stage between Eurasia and Africa (e.g. Dercourt et al., 1986; Dewey et al., 1989; Mazzoli and Helman, 1994; Handy et al., 2010; Frizon de Lamotte et al., 2011; Carminati et al., 2012; Faccenna et al., 2014) and by the subsequent back-arc overprint associated with the late Oligocene to Miocene opening of the Liguro-Provençal basin (e.g. Alvarez et al., 1974; Réhault et al, 1984; Hippolyte et al., 1993; Doglioni et al, 1997; Séranne, 1999; Gattacceca et al., 2007; Bache et al., 2010; Jolivet et al., 2015; Granado et al., 2016). As a result of this deformation history, the Briançonnais is exposed in the Western and Central Alps, whereas relics of the Valais "ocean" occur in the easternmost Western Alps and further east, in the Central and Eastern Alps (Schmid et al., 2004); the Corsica-Sardinia form an independent block (Fig. 3). Albeit all these uncertainties, information about the eastern termination of the Iberia-Eurasia plate boundary can be obtained from the occurrence and orientation of Cretaceous extensional structures in this area, along with their

6

affinity with structures of the western and central portions of the Iberia-Eurasia plate boundary. These features can provide robust insights on the eastern termination of the plate boundary.

The main goal of our work is to present both new information and reappraisal of published data about the mid-Cretaceous geological framework of this area and evaluate its kinematic compatibility with the mid-Cretaceous structures of the Pyrenean rift.

### 1.2 An overview of the Cretaceous Iberia-Eurasia plate boundary

The westerly Bay of Biscay arm includes a central area made of oceanic crust with an 83 Ma fossil ridge, in between the northern (European) and southern (Iberian) continental margins (Tugend et al., 2014, 2015). These margins are made of thinned continental crust and exhumed mantle (e.g. Boillot et al., 1979; Thinon et al., 2002; Cadenas and Fernández-Viejo, 2017) (Fig. 3b). Whereas the northern margin has persisted broadly undeformed since the end of rifting, the southern margin has been severely deformed by Late Cretaceous to Cenozoic compressional deformation (e.g. Roca et al., 2011; Pedreira et al., 2015). To the east the Mesozoic Iberia-Eurasia plate boundary continues into the Pyrenean arm (Fig. 3b). The Pyrenean arm was constituted by a segmented rift system formed by partly interconnected basins that have been inverted and incorporated into the Pyrenean mountain belt (Fig. 3a) during the Late Cretaceous to Cenozoic convergence between Iberia and Eurasia (e.g. Puigdefabregas and Souquet, 1986; Roure et al., 1989; Muñoz, 1992; Teixell, 1998; Vergés et al., 2002; Mouthereau et al., 2014). Despite the significant compressional overprint, the original architecture of the Pyrenean arm is still recognisable (Fig. 3b). Exposures of subcontinental lithospheric mantle exhumed by the end of the Cretaceous rifting have been reported for a long time in the Pyrenees (e.g. Lacroix, 1895; Vielzeuf and Kornprobst, 1984; Lagabrielle and Bodinier, 2008; Jammes et al., 2009; Lagabrielle et al., 2010; Masini et al., 2014; Clerc et al., 2015). These exposures occur along a narrow WNW-ESE elongated ribbon (Fig. 3b), flanked to the north and to the south by Late Jurassic to mid-Cretaceous basins of the European and the Iberian continental margins (e.g. Souquet et al., 1985; Lanaja, 1987; Rat, 1988; Johnson and Hall, 1989; Debroas,

414
415
416
417
418
419
420
421
422
423
424
425
426
427
428
429
430
431
432
433
434
435
436
437
438
439
440
441
442
443
444
445
446
447
448
449
450
451
452
453
454
455
456
457
458
459
460
461
462
463
464
465
466
467
468
469
470
471
472

1990; Cámara, 1997; García-Senz, 2002; Muñoz, 2002; Vergés et al., 2002; Tavani and Granado, 2015; Teixell et al., 2016). To the west, these basins and the exhumed mantle exposures are segmented by major transfer zones, namely the Santander and Pamplona faults (e.g. Roca et al., 2011; Tugend et al., 2014) which run broadly perpendicular to the orientation of the extensional basins (Fig. 3b). The eastern limit of subcontinental mantle exposures is located a few tens of kilometres to the west of the Mediterranean Sea coastline, and is thus considered the eastern termination of the Pyrenean Arm. Further to the east-northeast, Cretaceous extensional deformation is reported in the Provence region (e.g. de Graciansky et al., 1987; Hibsch et al., 1992; Montenat et al., 1997; Homberg et al., 2013). The Provence constitutes the easternmost portion of the Pyrenean orogenic system (Fig. 3a). In this easterly sector, a set of inherited Paleozoic to Mesozoic NNE-SSW to NE-SW striking transverse faults occur (Fig. 3b), i.e. the Cévennes, Nimes, and Durance-Aix faults from west to east (Masse and Philip, 1976). During the Late Cretaceous to Cenozoic time interval, these faults have provided the left-lateral transpressive junction between the E-W trending and north-verging Pyrenean structures of the Pyrenees and of the Languedoc-Provence region (e.g. Mauffret and Gennesseaux, 1989; Séranne et al., 1995; Lacombe and Jolivet, 2005; Molliex et al., 2011; Bestani et al., 2016) (Fig. 3a). Concerning the pre-contractional activity of the NNE-SSW to NE-SW striking Cévennes, Nimes, and Durance-Aix faults, several authors such as de Graciansky and Leimone (1988) and more recently Masse et al. (2009), have documented major WNW-ESE striking Early to mid-Cretaceous normal faults bounded by NNE-SSW to NE-SW striking transfer faults in the Provence region (Fig. 3). Given that the NNE-SSW to NE-SW striking transfer faults of this area are oriented about parallel to the major transfer faults that segment the Bay of Biscay-Pyrenean rift system (i.e., Pamplona and Santander faults), the easterly Provence region shares a structural similarity with the Bay of Biscay-Pyrenean rift system. In this work we propose that this series of transversal faults played a major role during rifting between Iberia and Eurasia, acting as transform zones that accommodated rift segmentation, and transferred the extensional deformation to the NE of the Pyrenean arm of the rift (Fig. 3c). In agreement with our working hypothesis, we

8

also present field survey data from an area that we consider the easternmost remanence of the Cretaceous Iberia-Eurasia plate boundary: the Marguareis area of the Briançonnais domain.

The presentation of data in the next sections is organised as follows: we first provide a review on the timing and kinematics of the various basins of the Pyrenean Arm (Section 2) and of the area comprised between the easternmost portion of the Pyrenees and the Provence region (Section 3). Finally, in Section 4, we introduce the Marguareis extensional system. The provided comprehensive review about the Cretaceous extension recorded to the east of the Bay of Biscay-Pyrenean rift allows us to propose that the Marguareis extensional system represents the easternmost structure of the segmented Bay of Biscay-Pyrenean rift. At the light of the work carried out in the Marguareis area, we discuss the three possible scenarios previously introduced for the development of the Bay of Biscay-Pyrenean rift and its eastwards continuation during the mid-Cretaceous.

## 2 An overview of the Pyrenean Arm

The westernmost sector of the Iberian-Eurasian plate boundary is constituted by an E-W trending fossil oceanic ridge, located on the abyssal plain of the Bay of Biscay (Fig. 3b), and inactive since early Campanian times (e.g. Sibuet et al., 2004; Roca et al., 2011). The oceanic ridge is flanked to the north and to the south by Aptian-Albian to Campanian oceanic crust (Figs. 3b, 4) (Tugend et al., 2014). The domain of oceanic crust fades out towards the north, the south, and the east into a domain of sub-continental mantle exhumed during Barremian to Aptian times (Thinon et al., 2003; Roca et al., 2011). The V-shaped Bay of Biscay wedges out toward the east, where it terminates into the E-W elongated Parentis basin (Fig. 4), which is filled by as much as 8 km of Upper Jurassic to Albian synrift sedimentary rocks (e.g. Ferrer et al., 2008). The southern margin of the Bay of Biscay includes an emerged area with small exposures of the Upper Jurassic to Lower Cretaceous synrift sequence (named Asturian basin by Lepvrier and Martínez-García, 1990). In these small-sized areas, the background fracture pattern indicates a synrift NNE-SSW oriented

9

extension (Site 1 of figure 4a) (Granado et al., in press).

The Santander Transfer Fault and the Landes Plateau divide the Bay of Biscay and the Pyrenean arms. The latter during the Cretaceous was occupying the area presently comprised between the Santander Fault to the west and the southern prolongation of the Cévennes Faults to the east (Fig. 4a) (e.g. Tugend et al., 2014). In this area, the Late Jurassic-Early Cretaceous extensional structures belonging to the Pyrenean Arm of the rift have been inverted and incorporated into the Pyrenean belt. These extensional structures include major lithospheric-scale shear zones that were responsible for the development of the continental margin basins (e.g. Souquet et al., 1985; Rat, 1988; Debroas, 1990; Muñoz, 2002; Vergés et al., 2002) and, ultimately, for the exhumation of sub-continental lithospheric mantle (e.g. Johnson and Hall, 1989; Jammes et al., 2009; Clerc and Lagabrielle, 2014; Tugend et al., 2014; Masini et al., 2014; Teixell et al., 2016); no oceanic crust has ever been documented in the Pyrenean Arm. The along strike structural variations of the Pyrenees are as well controlled by the inherited segmented configuration of the Bay of Biscay-Pyrenean rift system, with major NNE-SSW transfer zones striking roughly perpendicular to the main extensional basins.

Based on the lateral continuity of such extensional domains, the Pyrenean Arm has been further divided into two portions separated by the lithospheric-scale Pamplona transfer fault (Fig. 4) (e.g. Muñoz, 2002). The Basque-Cantabrian basin forms the westernmost portion of the Pyrenean rift (Fig. 4a). It has an overall E-W elongated shape and it is filled by up to 10 km thick Upper Jurassic to Albian/Cenomanian synrift infill (e.g. García-Mondéjar et al., 1986; Rat, 1988). The Basque-Cantabrian basin is bounded to the west by the N-S trending Santander transform fault (Roca et al., 2011) and to the east by the Pamplona fault (Fig. 4a), an inherited Paleozoic structure that acted as a transform fault during rifting (e.g. Rat, 1988; Larrasoaña et al., 2003). In the Basque-Cantabrian basin, multiple Late Jurassic to Early Cretaceous local extension directions are recorded by meso-structures (Tavani and Muñoz, 2012) and inferred from studies of anomaly of magnetic susceptibility (AMS; Soto et al., 2008; Oliva-Urcia et al., 2013; Site 2 in figure 4a). The dominant

591
592
593
594
595
596
597
598
599
600
601
602
603
604
605
606
607
608
609
610
611
612
613
614
615
616
617
618
619
620
621
622
623
624
625
626
627
628
629
630
631
632
633
634
635
636
637
638
639
640
641
642
643
644
645
646
647
648
649

synrift extension direction provided by these studies is roughly NNE-SSW (Site 2 of figure 4a) (Tavani and Muñoz, 2012), which is nearly parallel to the Santander transfer zone and perpendicular to the elongation of the basin.

A few tens of km to the south of the Basque-Cantabrian basin, the Cameros basin was forming part of a suite of Mesozoic extensional basins now exposed along the Iberian Chain (Figs. 3 and 4). These basins formed in the interior of the Iberian plate, disconnected from the Bay of Biscay-Pyrenean rift, along the NW-SE elongated Central Iberian rift system (e.g. Álvaro et al., 1979; Salas and Casas, 1993; Salas et al., 2001; Vergés and Garcia-Senz, 2001). The Central Iberian Rift contributed significantly to the continental separation between Iberia and Eurasia (Salas et al., 2001; Tugend et al., 2015). Analogously to the Basque-Cantabrian basin, extension direction recorded by meso-structures in the Upper Jurassic to Lower Cretaceous synrift sediments of the Cameros basin is NNE-SSW (Mata et al., 2001), whereas AMS studies provide two mutually orthogonal directions, corresponding to NNW-SSE to NW-SE and WNW-ESE to NE-SW (e.g. Soto et al., 2008; García-Lasanta et al., 2014) (Site 3 in figure 4a).

Immediately to the east of the Pamplona fault, the axis of mid-Cretaceous extension is shifted northward. Intense extensional deformation is recorded in the Arzacq and Mauléon basins, which are divided by the Grand Rieu ridge (Daignières et al., 1994; Teixell, 1988; Jammes et al., 2009, 2010; Masini et al., 2014; Teixell et al., 2016). The northerly Arzacq basin developed on the European plate and displays a rather simple E-W elongated sag-like geometry (e.g. Masini et al., 2014) with a Tithonian to Albian synrift infill (Biteau et al., 2006). Extensional deformation was more intense on the Mauléon basin to the south (e.g. Fortané et al., 1986; Johnson and Hall, 1989; Jammes et al., 2009; Lagabrielle et al., 2010; Masini et al., 2014), where sub-continental mantle was exhumed. The lithospheric extensional detachment system involved the Mesozoic sedimentary succession, crustal rocks, and upper mantle lherzolites. Measured S-C structures have indicated a top-to-the-north movement for the mantle-exhuming detachment (Lagabrielle et al., 2010) (Site 4 of figure 4a). Mesostructures studied by Salardon et al. (2017), which affect the sedimentary cover of

the Chaînons Béarnais area in the Mauléon basin (Site 5 of figure 4a), provide a similar N-S oriented extension direction for the Albian to Cenomanian interval. Similarly, Cretaceous N-S to NNW-SSE extension has been documented in the same area by Olivia-Urcia et al. (2010) by means of an AMS study. In the Mauléon basin, hyperextension and consequent exhumation of sub-continental mantle occurred during the late Aptian to Cenomanian interval (Jammes et al., 2009; Lagabrielle et al., 2010; Masini et al., 2014). The Arzacq-Mauléon system is bounded to the east by the NE-SW to NNE-SSW striking Toulouse fault. Many have proposed that this fault was acting as a transfer fault segmenting the Pyrenean Arm (e.g. Tugend et al., 2014), however, this is not fully demonstrated, and its possible segmenting role is by far less than that of the major transfer faults of the rift system. Relics of sub-continental mantle are exposed to the east and to the west of the Toulouse fault, occurring aligned in a WNW-ESE direction, with no remarkable shift across the fault. Domains of exhumed mantle and hyperextended crust are surrounded by Mesozoic sedimentary basins that have been incorporated into the Pyrenean belt (e.g. Lagabrielle et al., 2010; Tugend et al., 2014; Clerc et al., 2015). These basins, along with the Mauléon basin to the west, were initially developed isolated and became connected during the Albian-Cenomanian interval to form a large, WNW-ESE trending hyperextended basin (i.e. the Flysch Noir basin in figure 4) filled by the syn-extensional Flysch Noir Formation (e.g. Souquet et al., 1985; Debroas, 1990). Direction of mid-Cretaceous extension was N-S to NE-SW, as provided by major extensional detachments exposed in the Variscan massifs of the north Pyrenean area. These massifs constitute relics of the former crystalline basement of the various Cretaceous basins. In more detail, mid-Cretaceous extensional detachments associated with N-S to NNE-SSW oriented stretching are exposed in the Saint Barthélémy massif area (Site 6 of figure 4a) (Passchier, 1984; de Saint Blanquat et al., 1986; 1990) and in the Agly Massif (Site 7 of figure 4a) (Vauchez et al., 2013).

To the south of the Flysch Noir basin, the Organyà basin developed onto the Iberian crust. The Tithonian/Berriasian to middle Albian synrift sequence of the Organyà basin exceeded 4 km (Dinarès-Turell and García-Senz, 2000; Garcia-Senz, 2002), with a thickness distribution

characterised by a marked E-W to WNW-ESE elongated shape (Garcia-Senz, 2002; Mencos et al., 2015). Anisotropy of magnetic susceptibility (AMS; Gong et al., 2009; Olivia-Urcia et al., 2011) and meso-structural studies (Tavani et al., 2011) have been independently carried out in the area. The AMS works provide partly contrasting results, with Gong et al. (2009) suggesting a mainly N-S directed extension during rifting and Olivia-Urcia et al. (2011) recording a more scattered pattern for the AMS. In agreement with Gong et al. (2009), meso- and macro-structures (including syn-sedimentary faults) documented by Tavani et al. (2011) indicate N-S to NNE-SSW oriented basin-scale Early Cretaceous extension (Site 8 of figure 4a), which was perpendicular to the above mentioned basin axis.

**3 Cretaceous extension along the eastern portion of the Iberia-Eurasia boundary**

In this section we review the Late Jurassic to Cretaceous extensional structures reported in the area comprised between the easternmost portion of the Pyrenees and the Provence belt, in Sardinia, and in the European paleo-margin of the Western and Central Alps (Fig. 3a). In the previous section we have illustrated extensional structures involving the basement, and thus having an indisputable tectonic origin, whereas we have not included in our description the gravitational structures occurring in the Pyrenean arm (López-Mir et al., 2015; Saura et al., 2016). In this section we continue to report only on structures that, due to their regional size or because of the lack of evaporites (or any kind of mobile unit), cannot be interpreted as gravitationally-induced.

3.1 Eastern Pyrenees

The easternmost portion of the Pyrenean mountains is characterised by the termination of the Pyrenean basins (Fig. 5a). During convergence, the area around the Corbières Transfer Zone (e.g. Souque et al., 2002; Luis et al., 2006; Rouvier et al., 2012) became the left-lateral transpressive junction between the north-verging Pyrenean structures of the Pyrenees and the Provence region (Fig. 3a), as shown by Mauffret and Gennesseaux (1989), Séranne et al. (1995), Lacombe and Jolivet (2005) and more recently by Rouvier et al. (2012). Despite the contractional overprinting,

thickness variations of the Jurassic-Cretaceous sequence partly illustrate the rift architecture of the area. In detail, the Boucheville, Bas Agly and St. Paull de Fenouillet synclines to the north of the North Pyrenean Fault, are remanences of the easternmost mid-Cretaceous interconnected and hyperextended basins of the Pyrenean Arm separating Iberia from Eurasia (e.g. Lagabrielle et al., 2010; Tugend et al., 2014; Clerc et al., 2015). As previously mentioned in section 2, during the Albian-Cenomanian interval these basins were forming a large WNW-ESE trending trough, filled by the synrift Flysch Noir Formation (e.g. Souquet et al., 1985; Debroas, 1990). Extension beneath the Boucheville basin reached full crustal thinning and mantle exhumation, as indicated by the occurrence of peridotite bodies and the thermal metamorphism affecting the Mesozoic prerift and synrift sequences (Clerc et al., 2016). Regionally speaking, the synrift package in this area wedges out northward, to the north of the North Pyrenean Fault (Figure 5a). Indeed, the Mesozoic sequence in the Mouthoumet massif is represented only by postrift Upper Cretaceous strata resting on top of the Paleozoic basement (Fig. 5a). To the west of the NNW-SSE striking Cévennes fault, the area between the Mouthoumet and Montagne Noire massifs was also uplifted during the mid-Cretaceous, as indicated by the reduced thickness or complete lack of Lower Cretaceous units (e.g. Ellenberger, 1967; Souque et al., 2002). The thickness of the Lower Cretaceous is instead in the order of one km in the Bas Agly syncline (Fig. 5b), where a major mid-Cretaceous N-ward directed extensional detachment is exposed (Vauchez et al., 2013). Exposures of Lower Cretaceous sediments continue from the Bas Agly syncline toward NE, in the La Clape area of the Corbières thrust sheet (Fig. 5a), where the Mesozoic sequence is about 4 km thick, and the thickness of the Lower Cretaceous sediments alone is nearly one km (Deville et al., 1994). As previously indicated, such thickness decreases from the La Clape area toward the west across the south-western prolongation of the Cévennes fault; this is a clear evidence of the key basin-bounding role of the southern prolongation of the Cévennes fault during the mid-Cretaceous.

On the southeastern side of the Pyrenees, the Figueres-Montgrí basin is the easternmost exposed Lower Cretaceous basin in the Iberian Peninsula (Fig. 5a). It is an understudied structure,

14

827
828
829
830
831
832
833
834
835
836
837
838
839
840
841
842
843
844
845
846
847
848
849
850
851
852
853
854
855
856
857
858
859
860
861
862
863
864
865
866
867
868
869
870
871
872
873
874
875
876
877
878
879
880
881
882
883
884
885

only rarely referred and briefly described in the literature (e.g. Pujadas, et al., 1989; Tassone et al., 1994; Vergés et al., 2002). The thrust sheet involving the Figueres-Montgrí basin has been dismembered by Neogene NW-SE extensional faults at a transfer zone linking the Gulf of Lion and Valencia Trough rift system during the Oligocene-Eocene opening of the Western Mediterranean (Fig. 5a). Available geological data about the Figueres-Montgrí basin are provided by the published 1:25000 geological maps of Catalunya (Saula et al., 1994; Mató et al., 1995a,b; Pi et al., 1997). The Figueres-Montgrí thrust sheet includes two major portions exposed near the Figueres and Torroella de Montgrí villages (Fig. 5a). From a structural point of view, the Figueres-Montgrí thrust sheet involves a Mesozoic sedimentary succession including Triassic, Jurassic and both Lower and Upper Cretaceous strata (Fig. 5a). The thrust sheet has been transported out-of-sequence during the Late Eocene-Early Oligocene to the S or SW over another thrust sheet carrying a thin Mesozoic package of Jurassic and Upper Cretaceous strata with a significant absence of synrift sediments. This thrust sheet, named Bac Grillera-Biure thrust sheet (Pujadas et al., 1989), was transported to the south during the Paleocene-Early Eocene on top of a basement involved thrust sheet characterised by Paleocene red beds unconformaby overlying the pre-Variscan basement. The Bac Grillera-Biure thrust sheet is folded by Axial Zone antiformal stack and connects to the north with the hanging wall of the Banys d'Arles thrust south of the North-Pyrenean Fault (Fig. 5). The Figueres-Montgrí thrust sheet therefore, brings a Lower Cretaceous synrift basin over the basin's postrift Upper Cretaceous margin (Pujadas et al., 1989), which was in continuation with the axis of the Pyrenean rift arm. The Lower Cretaceous sequence within Figueres-Montgrí basin is more than 2 km thick (Saula et al., 1994; Mató et al., 1995a) and resembles the one observed in the Corbières thrust sheet (Fig. 5). It rests paraconformably on top of Jurassic carbonates and it is unconformably overlain by Upper Cretaceous strata (Mató et al., 1995b). In more detail, the Aptian-Albian succession is up to 2 km thick, evidencing a major Early Cretaceous subsidence stage. Unconformities and syn-sedimentary faults indicate a synrift stage for this basin. The easternmost portion of the Figueres-Montgrí basin crops out in the Medas islands (Fig. 5c), where NW-SE striking extensional faults

15

affect Hauterivian to Berriasian layers and are sealed by unconformable Aptian strata (Fig. 5c) (Mató et al., 1995b). Another important unconformity is observed in the onshore Figueres area, where Cenomanian strata are unconformable on Aptian and Albian units (Fig. 5d). Altogether, these observations indicate that: (i) onset of extension occurred between the Barremian and Aptian age, (ii) the oldest post rift unit is Cenomanian in age, (iii) syn-sedimentary faults (observed in the Meda islands) point to a NW-SE oriented structural trend for the Figueres-Montgrí basin.

3.2 SE France basin

This is the area comprised between the easternmost portion of the Pyrenees and the foreland of the Western Alps (Fig. 6), where Late Jurassic to Late Cretaceous extensional structures are known for a long time (e.g. Cotillon, 1968; de Graciansky and Lemoine, 1988). The SE France basin (Fig. 6b) originated on the European continental crust during the Triassic-Jurassic interval in response to Gondwana break-up and Alpine Tethys rifting (Lemoine, 1984; Curnelle and Dubois, 1986). Isopachs and facies distribution of Triassic, Lower and Middle Jurassic units in the basin are NE-SW elongated. This direction is parallel to the former Tethyan palaeomargin (Curnelle and Dubois, 1986) and defines a Triassic to Middle Jurassic through, positioned along the southwestern prolongation of the Valais ocean; no evidence for an oceanic substratum in this area have been reported. Starting from the Late Jurassic, the structural trend of the area became E-W. Indeed, the observed facies distribution allowed defining two Late Jurassic to Cretaceous E-W elongated sub-basins within the SE France basin: the Vocontian basin and the South Provence basin (Curnelle and Dubois, 1986). These sub-basins were separated by the also E-W striking Durance Isthmus, which became aerially exposed during the Cenomanian (Fig. 6b).

The Vocontian basin is largely exposed, whereas the mid-Cretaceous South Provence basin (e.g. Philip, 1970; Philip et al., 1987) has only few onshore exposures. One of them is the Beausset syncline (Fig. 6b), where the southern boundary of the basin occurs (Hennuy, 2003). The uplift stage which led to the division of the Vocontian and South Provence basins, commonly referred to as the "Durance Uplift" event, has occurred in an extensional framework. This is evidenced by mid-

16

945
946
947
948
949
950
951
952
953
954
955
956
957
958
959
960
961
962
963
964
965
966
967
968
969
970
971
972
973
974
975
976
977
978
979
980
981
982
983
984
985
986
987
988
989
990
991
992
993
994
995
996
997
998
999
1000
1001
1002
1003

Cretaceous syn-sedimentary extensional faults coeval with uplift and bauxite formation and sealed by Turonian strata (Guyonnet-Benaize et al., 2010). Coeval extensional faulting is documented southward, at the southern margin of the South Provence basin. There, Cenomanian strata unconformably overlie Berriasian to Albian strata defining an Albian half-graben associated with a roughly E-W striking fault (Fig. 7a). However, the onset of extension in the SE France basin is dated back at least at the Berriasian-Valanginian interval; this is documented by Valanginian strata unconformably resting on top of Berriasian strata folded by block-tilting associated with WNW-ESE striking extensional faults (Masse et al., 2009). Meso-structural data point to an extensional regime for the area too, with the Late Jurassic to mid-Cretaceous interval being characterised by extension directions roughly N-S to NNE-SSW and E-W to WNW-ESE oriented (e.g. Guyonnet-Benaize et al., 2010; Lamarche et al., 2012; Homberg et al., 2013), with a minor strike-slip contribution (e.g. Hibsch et al., 1992; Montenat et al., 1997). The link between the N-S and E-W oriented extensional structures and strike-slip deformation is recognised in the whole area also at more regional scale of observation (de Graciansky and Lemoine; 1988) (Fig. 6c). In agreement with the data reviewed above, the structural framework reported by these authors for the Early Cretaceous interval includes: major basin-scale WNW-ESE striking extensional faults associated with NNE-SSW oriented extension (Sites 10 in figure 8a); secondary NNE-SSW trending transverse extensional faults occurring in the hanging wall of major faults; NNE-SSW striking transfer strike-slip faults. The trend of the strike-slip set recognised by de Graciansky and Lemoine (1988) is parallel to the strike of the major inherited faults of the area, i.e. Cévennes, Nimes, and Durance-Aix faults. Such a framework, in which the above-mentioned faults acted as transfer systems, is confirmed when linking this area with the eastern Pyrenees. In this sense, during mid-Cretaceous times, the Vocontian basin was clearly delimited westward by the Cévennes fault (Fig. 6b). The same fault seems to confine the South Provence basin too (Fig. 6b): the Bas Agly syncline, which forms the easternmost relic of the suite of mid-Cretaceous basins of the Pyrenean mountains, (e.g. Vauchez et al., 2013; Clerc et al., 2016), is shifted southward with respect to the South

17

Provence basin. The Corbières transfer zone (Fig. 5a) thus acted either as a soft- or hard-linked transfer zone (Gawthorpe and Hurst, 1993) during the mid-Cretaceous times, roughly coinciding with the SW continuation of the Cévennes fault.

3.3 Sardinia

In the Sardinia-Corsica block to the south of the South Provence basin (Fig. 6a), a structure similar to those described by Guyonnet-Benaize et al. (2010) for the South Provence basin also points to coeval uplift and block tilting. This structure occurs in the Olmedo area of NW Sardinia (e.g. Mameli et al., 2007) (Fig. 7b), where Coniacian strata unconformably overly a tilted sequence of Berriasian to Aptian sediments with bauxite bodies at the top. This configuration evidences tilting during mid-Cretaceous times, with the pre-unconformity monocline dipping to the SE. By removing the 95° of Cenozoic clockwise vertical axis rotation of Sardinia (Advokaat et al., 2014), this configuration corresponds to a roughly SW-dipping monocline in a Cretaceous reference framework (Site 11 in figure 8a).

3.4 Western and Central Alps

The Helvetic Domain of the Central Alps corresponds to the Mesozoic European continental margin of the Alpine Tethys. In this area, extensional faults postdating the Alpine Tethys rifting stage have been reported at different time intervals. Septfontaine (1995) described a Late Jurassic extensional system (Site 12 in Figure 8a) constituted by a reactivated WSW-ENE striking Early Jurassic fault that developed during Tethyan rifting. The late Jurassic reactivation of this fault is evidenced by the occurrence of an about 500 m-wide NW-ward thickening growth wedge of Upper Jurassic strata. In the same region, Cardello and Mancktelow (2014) report Cretaceous extensional structures at cm to km scales (Site 13 of figure 8a). Evidence of Late Cretaceous extensional deformation includes growth wedges, sedimentary dykes, thickness and facies variations, palaeoescarpments, and slump folds. All these features are related to km-sized SW-NE-striking faults developed in response to Santonian to early Maastrichtian NW-SE extension (Cardello and Mancktelow, 2014), oriented perpendicular to the Tethyan palaeomargin. Timing and direction of

extension recognised in both areas are not in line with those previously described in sections 2 and 3 (Fig. 8b). In addition, Cardello and Mancktelow (2014) have suggested a possible gravitational origin for these structures. For those reasons, these structures are not considered as forming part of the Iberia-Eurasia rift system.

In the External Briançonnais Domain of the Western Alps, Late Jurassic to Cretaceous extensional structures have been reported also (e.g. Chaulieu, 1992; Claudel et al., 1997; Claudel and Dumont, 1999). A WSW-ENE striking Callovian-Oxfordian extensional fault reactivated during Albian and Turonian and a NW-SE striking Albian fault were described by Claudel et al. (1997) (Site 14 of Figure 8). Claudel et al. (1997) also reported the occurrence of mid-Cretaceous condensed sections, stratigraphic gaps, angular unconformities and neptunian dykes; all these features are evidence for mid-Cretaceous extensional tectonics in the area. Similar observations have been made by Chaulieu (1992), who inferred an Albian-Turonian extensional reactivation of inherited Tethyan faults based on the occurrence of chaotic breccias along with several Jurassic faults. According to this, the External Briançonnais Domain of the Western Alps area (Site 14 in figure 8a) recorded an extensional pulse accompanied by uplift and erosion during Aptian to Turonian times. Contrary to the nearby SE France basin, Helvetic domain, and eastern Pyrenees, the direction of extension is not provided for the External Briançonnais Domain of the Western Alps, because this area underwent significant - and variable - counter-clockwise vertical axis rotation with respect to the stable Europe framework during Cenozoic times (Collombet et al., 2002).

Finally, in the Marguareis Extensional System of the Western Alps, Bertok et al. (2012) reported mid-Cretaceous extension (Site 15 in Fig. 8a). In the next section, we illustrate how the Marguareis area underwent extension between the Valanginian to Aptian and the early Late Cretaceous, accompanied by block tilting.

3.5 Summary of the eastern Iberia-Eurasia boundary

The link between the structures described in the eastern Iberia-Eurasia boundary and those

19

from the Bay of Biscay – Pyrenean rift system (described in section 2) is evident when comparing timing and direction of extension for both areas (Fig. 8b). Although the onset of extension in the Pyrenean Arm is slightly older, end of extension by mid-Cretaceous times is almost coeval in the Pyrenean Arm to the west, in the Vocontian and South Provence basins, and in the External Briançonnais of the Western Alps. It is noticeable that the Cévennes fault is almost parallel to the transfer faults of the Pyrenean arm. In addition, the directions of extension to the east and to the west of this fault are parallel to each other, and roughly parallel to the strike of the fault, across which the mid-Cretaceous depocenters are shifted. All these features evidence that the Cévennes fault acted as - or was forming the most important part of - a transfer zone during mid-Cretaceous extension.

## 4. Introducing the Marguareis Extensional System

The Cretaceous Marguareis extensional system is located at the SW termination of the Western Alps (Ligurian Alps, Fig. 9a), in the eastern part of the External Briançonnais Domain. The Briançonnais Domain is considered a major palaeogeographic domain and a tectonic unit of the Western Alps (Schmid et al., 2004 and references therein) (Fig. 3b).

### 4.1 Geological overview

The Western Alps formed during the collision between the Adria and the European continental margins of the Alpine Tethys ocean, following the Late Cretaceous to Eocene subduction of this ocean (e.g. Dercourt et al., 1986; Coward and Dietrich, 1989; Schmid and Kissling, 2000; Froitzheim et al., 2008; Handy et al., 2010; Faccenna et al., 2014). In the Western Alps, mountain building started during Early Eocene, when N-S convergence between Adria and Europe led part of the distal European continental margin and the Alpine Tethys oceanic lithosphere, i.e. the internal Alpine units, to be subducted southward below the Adriatic lithosphere, reaching HP- to UHP-metamorphic conditions (Goffé and Chopin 1986; Michard et al., 2004; Beltrando et al., 2007; Bousquet et al., 2008). During the Middle-Late Eocene, the metamorphosed internal units were exhumed and placed on top of the European continental margin as the North

20

Alpine Foreland basin was formed and progressively migrated toward the external sectors of the Alpine foreland (Ford et al., 2006; Malusà et al., 2011; Schlunegger and Kissling, 2015). A major change occurred in the Early Oligocene, when the motion of Adria with respect to Europe changed from N-ward to WNW-ward (Schmid et al., 1996; Handy et al., 2010; Dumont et al., 2012). This imposed a westward indentation of Adria that in the SW Alps produced the anticlockwise rotation of the Alpine units with respect to stable European lithosphere (Thomas et al., 1999; Schmid and Kissling, 2000). In the study area such an anticlockwise rotation was up to 120° (Fig. 9a) (Collombet et al., 2002), and led to a generalised left-lateral transpressional regime (Ford et al., 2006). As a consequence, SW-ward overthrusting of the internal units onto the external ones took place (Kerckhove 1969; Merle 1982; Coward and Dietrich, 1989; Fry, 1989; Michard et al., 2004; Dumont et al., 2011, 2012), together with the left-lateral juxtaposition of units initially belonging to different tectonic domains (Lemoine et al., 2000; Ford et al., 2006; Piana et al., 2009; d'Atri et al., 2016).

In the Western Alps, four adjacent Mesozoic palaeogeographic domains have been classically distinguished (Fig. 9a). From the internal (eastern in a Mesozoic reference framework) to the external (western in a Mesozoic reference framework) sectors, these domains are: the Piedmont-Ligurian Domain, corresponding to the Alpine Tethys Ocean, and the "Pre-Piemontese", Briançonnais, and Dauphinois-Provençal domains, corresponding respectively to the distal, inner and innermost part of the European Mesozoic continental margin (Lemoine et al., 1986). The Briançonnais units exposed in this area are classically further divided into internal and external units (Fig. 9a), mainly on the basis of their metamorphic features. The internal Briançonnais units were strongly affected by Alpine metamorphism, locally reaching HP- to UHP-LT conditions (Goffé and Chopin 1986; Michard et al., 2004; Beltrando et al., 2007; Bousquet et al., 2008). Conversely, only low-grade to anchizonal metamorphism developed in the external Briançonnais units (Piana et al., 2014; d'Atri et al., 2016, and references therein), where the Marguareis extensional system is located (Fig. 9).

21

The present-day structural setting and the relationships between the different tectonic units of the Marguareis area are mainly controlled by the WNW-ESE Limone-Viozene transpressive shear zone (Piana et al., 2009; d'Atri et al., 2016). This zone developed during the above-mentioned Alpine left-lateral strike-slip stage and produced the SW-ward transpressive re-imbrication of the external Briançonnais rocks onto a stack made of the buried Dauphinois-Provençal foreland succession, tectonically capped by the Helminthoides Flysch units of the internal Piedmont-Ligurian Domain. The major Alpine tectonic contact of the area is a transpressive fault that put in contact the Mesozoic sedimentary sequence of the Briançonnais domain to the north with the Helminthoides Flysch to the south (Fig. 9b). The external Briançonnais unit to the NE of this main contact is further divided into the Limone-Viozene Zone and the Marguareis Unit, to the south and to the north, respectively (Fig. 9b), the boundary corresponding to the Limone-Viozene northern boundary fault (d'Atri et al., 2016), hereinafter called LIVZn Fault. The Marguareis Unit in turn includes a western, central and eastern domain divided by N-S striking faults, as later detailed. The Limone-Viozene Zone (Piana et al., 2009; d'Atri et al., 2016) is defined as a regional WNW-ESE elongated tectonic unit extending for some tens of kilometres. In the study area, such a zone involves rocks of the external Briançonnais domain, and it is delimited by two main faults, namely the southern and northern Limone-Viozene boundary faults (Fig. 9b). These are arranged in a leading pattern, with the southern fault being the master structure dividing two different palaeogeographic domains. The northern one, i.e. the LIVZn Fault, is a trailing secondary structure, accounting only for less than a few km of left-lateral displacement, coherently with the fact that areas to the south and to the north of this northern fault share the same stratigraphy. Flower structures and highly deformed slices occur at the upper structural levels of the faults, i.e. where these affect the Upper Cretaceous to Cenozoic rocks. However, the LIVZn Fault in the study area is generally well-localised (as shown below), and its width spans from a few m up to some tens of m. As a result, the area in between the Limone-Viozene boundary faults, albeit the occurrence of some low displacement (i.e. <50 mt) faults, displays a rather simple large-scale synclinal geometry, with

22

1299
1300
1301
1302
1303
1304
1305
1306
1307
1308
1309
1310
1311
1312
1313
1314
1315
1316
1317
1318
1319
1320
1321
1322
1323
1324
1325
1326
1327
1328
1329
1330
1331
1332
1333
1334
1335
1336
1337
1338
1339
1340
1341
1342
1343
1344
1345
1346
1347
1348
1349
1350
1351
1352
1353
1354
1355
1356
1357

no significant internal deformation. In the following we will focus on the stratigraphy and structures of the Briançonnais units (i.e. Limone-Viozene and Marguareis tectonic units).

The oldest rocks exposed in the study area are volcanic and volcanoclastic rocks of Late Carboniferous-Permian age. These are overlain by a Lower Triassic to Upper Cretaceous sedimentary succession, which is subdivided into lithostratigraphic units mostly bounded by unconformities (Vanossi, 1969, 1972; Bertok et al., 2011) (Fig. 9b). From the bottom to the top, these are: (i) The "Quarziti di Ponte di Nava" Fm. (Upper Permian?–Lower Triassic?), which is constituted by continental to littoral conglomerates and cross-bedded quartz arenites, being locally interbedded with shales. This formation is about 200 metres thick in the study area. (ii) The "Dolomie di San Pietro dei Monti" Fm. (Anisian-Ladinian), which is made up by peritidal dolostones and limestones. Its top is truncated by an erosional surface corresponding to a hiatus which spans the Upper Triassic, Lower Jurassic and part of the Middle Jurassic. The thickness of this formation is variable in the study area, ranging from less than 500 up to 900 metres. (iii) The "Calcari di Rio di Nava" Fm. (Bathonian), consisting of monotonous dark micritic limestones deposited in a restricted carbonate shelf environment; the top is truncated by an erosional surface, locally associated with a slight angular unconformity. Its thickness ranges from few tens of metres up to about 150 metres. (iv) The "Calcari di Val Tanarello" Fm. (Kimmeridgian?–Berriasian): pelagic limestones locally exhibiting a nodular Ammonitico Rosso facies in the upper part, with a total thickness of some tens of metres. (v) The "Upega" Formation (Upper Cretaceous): grey hemipelagic marly limestones, separated from the underlying "Calcari di Val Tanarello" by a black crust of Fe-Mn oxides, glauconite and phosphates containing planktic foraminiferal assemblages referable to the middle Albian (Bertok et al., 2011). This mineralised hardground documents a prolonged hiatus encompassing the Valanginian-Aptian interval. The top of the Mesozoic succession is truncated by a regional unconformity, overlain by a Middle Eocene-Lower Oligocene Alpine Foreland succession, here composed of massive bioclastic limestones up to 30 metres thick, overlain by dark shales with interbedded turbiditic sandstone layers (d'Atri et al., 2016). In the

northeastern part of the Marguareis area the Cenozoic sediments directly rest on top of Jurassic limestones through an erosional surface. The Upper Cretaceous deep-water Upega Fm. is locally affected by a pervasive foliation, particularly nearby the Limone-Viozene boundary faults, which documents a strong localization of the deformation in anchizonal metamorphic conditions (Piana et al., 2014). Instead, the Permian-Jurassic stratigraphic succession experienced much less internal deformation, allowing for the preservation of most of the primary stratigraphic features (Piana et al., 2009; Bertok et al., 2011, 2012; Martire et al., 2014).

**4.2 Main faults of the Marguareis area**

Three major faults affect the Briançonnais units of the study area. The E-W-striking LIVZn Fault divides the Limone-Viozene zone to the south, where strata are SW-dipping, from the Marguareis Unit to the north. The latter unit is subdivided into the western, central and eastern domains, which are separated from each other by the N-S striking and E-dipping Colle del Pas and Passo delle Saline normal faults (Fig. 9b). Both faults extend for several kilometres and clearly abut upon the LIVZn Fault. The E-W striking LIVZn Fault in the western portion of the study area is near vertical and has W-dipping Mesozoic carbonates in the northern block and SSW-dipping to near vertical Permian volcanites and Triassic sediments in the southern block, respectively (Fig. 10a-c). The Principal Displacement Zone (PDZ; Tchalenko, 1970) is exposed to the NE of the Carnino Village (Fig. 10c-e), where the Middle Triassic "Dolomie di San Pietro dei Monti" Fm. is in contact with the Permian volcanites (Fig. 10c-d). The PDZ displays a left-lateral strike-slip kinematics (Fig. 10d, e). To the west, the LIVZn Fault has a N-ward dip of about 60°-70° and the PDZ is no longer well-exposed (Fig. 11). There the fault juxtaposes Cenozoic, Upper Cretaceous, and Jurassic rocks of the northern block, with Triassic and Jurassic to lowermost Cretaceous rocks of the southern block (Fig. 11a, b). At places the southern and northern blocks are 20-30 m apart, in other areas the LIVZn Fault is constituted by an up to 200 m wide zone including decametre- to hectometre-sized fault-bounded slices of Upper Cretaceous and Cenozoic rocks, arranged in an anastomosed geometry and stretched along an WNW-ESE direction. The southern block in this

western area is composed of a SSW-dipping monocline, which to the west is affected by left-stepping NW-SE striking and NE-dipping normal faults abutting on the LIVZ Fault (Fig. 11a, b), and showing displacement up to few tens of metres (Fig. 6a). In the northern block of the LIVZn Fault, a few tens of m apart from the fault itself, a Cretaceous E-W oriented palaeoescarpment has been documented by Bertok et al. (2012). This palaeoescarpment is evidenced by the occurrence of an irregular erosional surface incised within the Upper Jurassic - lowermost Cretaceous limestones of the Calcari di Val Tanarello Fm., locally covered by patches of a mineralised crust bearing planktic foraminifers assemblages referable to the Albian, and onlapped by the Upper Cretaceous sediments of the Upega Fm. (Fig. 11c-d). Close to the palaeoescarpment, metre- to decametre-sized olistoliths of Calcari di Val Tanarello limestones occur, completely embedded within the deep-water sediments of the Upper Cretaceous Upega Fm. (Bertok et al., 2012). It is worth noting that the palaeoescarpment does not correspond to the Cretaceous LIVZn Fault, as these structures have some orders of magnitude of difference: the LIVZn Fault affects the upper crust while the palaeoescarpment evidencing sub ordered faulting with less than a few tens of metres of displacement. The importance of the palaeoescarpments lies in the fact that they allow to constrain the age of the onset of extensional deformation.

The Passo delle Saline Fault, located in the eastern portion of the study area, runs almost N-S and abuts on the LIVZn Fault (Figs. 9b, 12a). The stratigraphic displacement of this fault is in the order of some hundreds of metres and the dip of the fault is 30° to 40° toward the east. Units exposed in both the hanging wall and the footwall dip toward the west. The Cenozoic sediments are not affected by extensional faults and in the hanging wall of the Passo delle Saline fault, they unconformably overlie the Triassic to Cretaceous sediments (Fig. 12a). N-S oriented extensional structures occur at different scales in the area. They span from the tens of km long Passo delle Saline and Colle del Pas faults, to the hundreds of m long extensional faults exposed in the hanging wall of the former fault (Fig. 12a) and includes also N-S striking background veins and joints, which are widespread in the Triassic and Jurassic carbonate beds (Fig. 12b).

25

To the west, the other N-S striking and E-dipping fault is the Colle del Pas Fault (Fig. 13). In its hanging wall, W-dipping Triassic and Jurassic carbonates are exposed. The footwall is made up of Permian to Jurassic rocks, dipping toward the west and, in the southern part, toward the south. Along the fault, the occurrence of sedimentary breccias unconformably resting on Permian volcanic rocks of the footwall, and onlapped by Upper Cretaceous sediments (Bertok et al., 2012) (Fig. 13b,c), evidence a Cretaceous normal displacement in the order of many hundreds of metres. Although most of the displacement has occurred before the deposition of the Upega Fm., the Colle del Pas Fault was still active at the beginning of the Late Cretaceous, as indicated by growth geometries in the lowermost portion of the Upega Fm. (Fig. 13d). Along the southern portion of the Colle del Pas Fault, the Piaggia Bella karstic system provides additional data about the fault geometry at depth (Fig. 13a). The karstic system is developed within the Mesozoic carbonates located on the hanging wall, which are juxtaposed to the impermeable base of the system, represented by the Permo-Triassic quartz arenites and shales of the Quarziti di Ponte di Nava Fm. and the Permian volcanic rocks, at the footwall. This tectonic contact between hanging wall carbonates and the impermeable base of the footwall is observed at several places along the karstic system (Fig. 14), and the corresponding XYZ coordinates are available. This subsurface dataset has been used for constructing the cross sections in figure 15.

**4.3 The 3D architecture of the Marguareis extensional system**

Field measurements of bedding, 5-m-resolution digital terrain model (DTM ICE 2009-2011 by Regione Piemonte), 0.5 m/px orthophotos (Orthoimages ICE 2009-2011 by Regione Piemonte), subsurface geological data from the Piaggia Bella karstic system, and geological maps by Vanossi (1972) and Bertok et al. (in Press), were integrated in the Midland Valley 3D Move software, in order to build a 3D model of the area. Ten representative vertical sections - six E-W and four N-S striking - are used to illustrate the 3D structure of the area (Fig. 15). All the E-W striking sections are from the northern block of the LIVZn Fault, and for all of them we reported: the distance between two pin lines placed at the edge of the section (computed at the top of Jurassic to

26

lowermost Cretaceous Calcari di Val Tanarello Fm.), the length of the unfaulted top of the Jurassic to lowermost Cretaceous, and the derived amount of extension. The amount of extension computed along all the E-W sections (including those in the 3D move file in the supplementary material) is also reported in the map on figure 15. A one-km long bar is provided for those sectors of the sections where, in 3D, the dip-direction of layers runs roughly parallel to the section, and its base is pinned at the base of the Quarziti di Ponte di Nava Fm. This bar thus serves to illustrate sedimentary thickness variations.

The E-W oriented sections to the north of the LiVZ are characterised by a domino pattern, with three main W-dipping blocks being bounded by the two major E-dipping Colle del Pas and Passo delle Saline extensional faults. In detail, the eastern and central tilted blocks dip about 20°, while the western one dips 30° (as seen in sections EW13, EW15, and EW17). The dip of N-S striking extensional faults, including the secondary ones, ranges between 30° and 45°, as seen also at depth along the Piaggia Bella Karstic system (Fig. 14), and their cutoff angles range between 50° and 60°. The amount of E-W extension to the north of the LIVZn Fault increases northward, being 21% close to the fault, and 38% in the northernmost E-W section. The extension is mostly achieved by slip along the two major faults, with a minor contribution from the other extensional structures. The slip along the Passo delle Saline Fault is roughly constant along its strike, whereas displacement along the Colle del Pas fault increases northward. The latter fault is thus responsible for the northward-increasing cumulative extension.

A first structural observation concerns the occurrence of a large anticline striking about WNW-ESE. To the west, in sections NS1 and NS4 of figure 15, the axis of the anticline is in the northern block of the LIVZn Fault. The northern limb of the anticline is tilted slightly, so the pre-folding geometries remain largely preserved. The anticline and the LIVZn Fault run oblique to each other and further to the east, along sections NS7 and NS10 of figure 15, the anticlinal axial surface is no longer occurring. The LIVZn Fault in this eastern area is near-vertical and displays a cutoff angle of about 90° with layers of its northern block. Cutoff angles with the folded layers of the

27

southern block range instead from 20° to 40°. The Quarziti di Ponte di Nava Fm. is about 150 to 200 m-thick in the entire area, with a couple of sections (western block of sections EW13 and EW7) in which its thickness reaches almost 300 m. A significant thickness variation of the Triassic Dolomie di San Pietro dei Monti Fm. is instead observed across the LIVZn Fault, being constantly below 600 m to the north and roughly 800-850 m to the south. Such a thickness variation is not accompanied by any remarkable structural repetition of the sequence, thus indicating its sedimentary origin. The total thickness of the Jurassic-lowermost Cretaceous formations spans between 150 and 250 m in the entire area. The original stratigraphic thickness of the Upega Fm. is hardly to assess due to the scarcity of outcrops of its upper boundary with the overlying Cenozoic sediments, the erosional nature of such boundary locally incising down to the Jurassic formations, and even because of the high finite strain affecting the Upega Fm. itself. Nevertheless, the geological map evidences that it is mainly preserved close to the N-S striking, E-dipping faults bounding westward the three main W-dipping blocks, and that it roughly wedges out toward the tilted blocks' culminations.

## 4.4 The Cretaceous structural framework

Observations provided in this work support the activity of the Colle del Pas and Passo delle Saline N-S striking normal faults during the Cretaceous. These faults form part of an extensional array that started to develop in the Valanginian-Aptian time interval, as indicated by Albian palaeoescarpments incised within the Upper Jurassic - lowermost Cretaceous limestones (Fig. 11c-d) (Bertok et al., 2012). The Upega Fm. mostly seals the extensional faults; however, we have documented that the lowermost portion of this unit includes growth geometries (Fig. 13d). Based on these observations, we deduce that extensional tectonics in the area spanned from the Valanginian-Aptian up to the early Late Cretaceous. The occurrence of metre- to tens of metres-sized olistoliths of Triassic dolostones and Jurassic limestones embedded within the Upper Cretaceous sediments, provide additional evidence for the Cretaceous extensional tectonics, as these features are coherent with the development of Cretaceous topographic highs and depocentres associated with extensional

28

tectonics. Along the Colle del Pas Fault, the Upper Cretaceous sediments locally onlap sedimentary breccias directly resting on an erosional surface incised within tilted Permian rocks (Fig. 13b,c). This documents a minimum normal displacement of the Cretaceous fault of about 700 metres, which is roughly equivalent to the present-day displacement. This demonstrates a roughly negligible Alpine overprint along this fault and suggests a similar framework for the Passo delle Saline Fault, where no evidence of inversion occurs. The domino pattern presently characterizing the area to the north of the LIVZn Fault is also interpreted as Cretaceous, as indicated by the breccia body resting on top of the Colle del Pas Fault. The fault is in fact dipping 30° eastward and has a cutoff angle of about 50-60°, assuming a Cenozoic tilting of the footwall of the Colle del Pas fault would require a Cretaceous breccias depositional angle of about 60 degrees, which is impossible.

The LIVZn Fault is characterised by an Alpine left-lateral displacement in the order of less than a few km. This value is suggested by scaling relationships between fault displacement and length (e.g. Cowie and Scholz, 1992; Kim and Sanderson, 2005). Indeed, these relationships point to less than a few km of displacement for a fault strand long less than a few tens of km, like the LIVZn. The marked thickness change of the Triassic sequence across it, indicates an at least Triassic origin, thus this fault was already formed during the Cretaceous. However, no direct observations on the Cretaceous kinematics and displacement of the WNW-ESE striking LIVZn Fault are presently possible, because of the above mentioned Alpine transpressive tectonics. The N-S striking Colle del Pas and Passo delle Saline faults abut against it and no N-S striking fault occur southward of the LIVZn Fault. These features support a kinematic relationship between the E-W striking LIVZn Fault and the Cretaceous N-S striking normal faults. As illustrated in figure 16, at Cretaceous times the restored NNE-SSW striking (once removed the 120º counter-clockwise rotation, Collombet et al., 2002), steeply dipping LIVZn Fault would have divided a westerly unfaulted block from an easterly faulted and southward translating extended block. This configuration implies that the LIVZn Fault was forming a hard-linked transfer fault (e.g., Gibbs, 1984; Morley et al., 1990; Gawthorpe and Hurst, 1993), with a right-lateral component as shown in

29

figure 16. Such transfer fault should extend much further the study area, as documented by the occurrence of other N-S striking faults (in present day orientation), both to the east (Mongioie Fault, Bertok et al., 2012) and to the west (Michard and Martinotti, 2002). Accordingly, we propose that during the Cretaceous the LIVZn Fault reached a total length of several tens of kms; however, no trustworthy information about the Cretaceous kinematics is available for this fault. Nevertheless, a series of NW-SE striking faults arranged in an en echelon pattern occurring in the western portion of the study area (Fig. 11a,b) could be taken as indicative for a Cretaceous right-lateral activity of the fault, albeit the timing of these en echelon faults is not constrained.

The last important observation concerns the sediments deposited during and after the faults activity. To the north of the LIVZn fault Upper Cretaceous sediments are mostly preserved within semi-graben basins related to the N-S striking faults. Their maximum thickness does not exceed 200 metres and they roughly wedge out toward the footwall scarp and the tilted blocks' culmination, where Cenozoic strata even directly rest on top of Jurassic carbonates. Olistoliths made up of Triassic and Jurassic carbonatic rocks occur embedded both within Upega Fm. and Cenozoic succession, thus proving that Late Cretaceous semi-graben basins were still under-filled in the Late Eocene.

Summarizing, the Valanginian-Aptian to early Late Cretaceous extensional system of the Marguareis area was characterised by a tens of kilometres long near vertical right-lateral fault (reactivating an inherited Triassic fault), whose strike was nearly NNE-SSW, having associated a set of normal faults, which accommodated an amount of SSW-directed extension in the order of some kilometres.


## 5 Discussion

Information provided in this work indicates that the Cretaceous structures of the Marguareis extensional system and the SE France basin are kinematically similar, and coeval to that of the Bay of Biscay - Pyrenean rift system. Our conclusion arises from the kinematic observations illustrated

30

above, coupled with information about timing of major geodynamic events. Data about the extension directions, the basins' shape and extensional domains, the orientation of transfer faults, and the timing of major tectonic events - i.e. basins formation and mantle exhumation - provide a consistent picture for a dominantly NNE-SSW oriented divergent movement along the Iberia-Eurasia plate boundary (Fig. 17). As discussed below, the plate boundary was formed by the Bay of Biscay and Pyrenean arms and, to the east of the Pyrenees, by the SE France Arm (made by the Figueres-Montgrí, South Provence, and Vocontian basins) and the Briançonnais Arm (made by the Marguareis extensional system) (Fig. 17b).

Transfer faults running perpendicular to major extensional faults and accommodating the connection between individual fault segments, faults, or extensional basins, are constitutive features of extensional systems (e.g. Gibbs, 1984; Morley et al., 1990; Lister et al., 1991; Gawthorpe and Hurst, 1993; Faulds and Varga, 1998), and include transform faults segmenting the actively spreading oceanic ridges (Wilson, 1965). A noticeable kinematic constraint at the Iberia-Eurasia plate boundary is provided by this kind of faults. All the major transfer faults segmenting the rift (i.e., Santander, Pamplona, Cérvennes, Durance-Aix, Nimes, and LIVZn faults) are roughly perpendicular to the WNW-ESE elongated Parentis, Basque-Cantabrian, Arzacq-Mauléon, Flysch Noir, Organyà, Vocontian, South Provence, and Marguareis basins, and are roughly parallel to the mid-Cretaceous extension directions recognised in all these areas (Fig. 17). This configuration admits very little, if any, obliquity in the rift system.

Timing of major events along the rift is slightly diachronic, overall pointing to an eastward propagation of the rift. The base of the synrift infill is Kimmeridgian in the Basque-Cantabrian basin (e.g. García-Mondéjar et al., 1986; Rat, 1988), Tithonian in the Arzacq basin (Biteau et al., 2006), and Tihtonian-Berriasian in the Organyà basin (Dinarès-Turell and García-Senz, 2000; Garcia-Senz, 2002) (Fig. 17b). The first evidence of extensional deformation to the east of the Cévennes fault is instead Early Cretaceous. In detail, it is Hauterivian to Berriasian in the Figueres-Montgrí basin (Mató et al., 1995b) and Berriasian-Valanginian in the SE France basin (Masse et al.,

1830
1831
1832
1833
1834
1835
1836
1837
1838
1839
1840
1841
1842
1843
1844
1845
1846
1847
1848
1849
1850
1851
1852
1853
1854
1855
1856
1857
1858
1859
1860
1861
1862
1863
1864
1865
1866
1867
1868
1869
1870
1871
1872
1873
1874
1875
1876
1877
1878
1879
1880
1881
1882
1883
1884
1885
1886
1887
1888

2009). In the Marguareis system to the east, onset of extension occurred between Valanginian and Aptian times. During the Albian-Cenomanian interval, the synrift stage ended in all the reviewed basins and hyperextension followed by the consequent exhumation of sub-continental mantle occurred in the Mauléon basin (Jammes et al., 2009; Lagabrielle et al., 2010; Masini et al., 2014). As already pointed out, the structures from the Central Alps have different timing and orientations instead (Fig. 8), and therefore may pertain to a different geodynamic framework, including gravitationally-induced deformation along the passive European margin of the Alpine Tethys ocean.

The kinematics, timing, and synchronicity of extensional deformation in the area extending from the Bay of Biscay to the External Briançonnais Domain, have major geodynamic implications for the long debated opening mode of the Bay of Biscay. The occurrence of roughly E-W elongated mid-Cretaceous basins to the east of the Cévennes fault, i.e., the Figueres-Montgrí, Vocontian, South Provence, and Marguareis basins, is incompatible with the scissor-type opening mode for the Bay of Biscay (Fig. 2). In that model, the mid-Cretaceous basins of the Pyrenees have been interpreted as back-arc structures (e.g. Sibuet et al., 2004). According to Advokaat et al. (2014), the mid-Cretaceous northward subduction of Iberia was confined eastward by a major N-S striking transform, located to the west of Sardinia (Fig. 2c). Such configuration cannot explain the occurrence of extensional deformation coeval with that of the Pyrenean arm, and to the east of the subduction termination. As mentioned in the introduction, the strike-slip opening mode assumes mid-Cretaceous transform plate boundary located along the North Pyrenean Fault. Eastward translation of Iberia would have accommodated to the east by the opening of the Valais ocean (e.g. Stampfli and Borel, 2002; Handy et al., 2010), which would represent a sort of dilation jog placed at the termination of a left-lateral transform fault. The mid-Cretaceous age of the Valais "ocean" is questionable in the light of U-Pb dating providing Early Carboniferous (Bussy et al., 2008), Permian (Beltrando et al., 2007), or even Late Jurassic (Liati and Froitzheim, 2006) ages. Moreover, the hypothesis of a mid-Cretaceous dilation jog of a hypothetical North Pyrenean transform fault is not supported by the data presented here and discussed as follows: after restoring the Corsica-

32

Sardinia block to its position before the opening of the Liguro-Provençal basin (Bache et al., 2010) (Figs. 3b, 6a), the block must be shifted southward tens of km to remove the Pyrenean shortening. Bestani et al. (2016) propose that Sardinia and Provence were 140 km apart before onset of Pyrenean convergence. Such a great distance allows placing a hyperextended continental crust or exhumed mantle domain, or even oceanic crust, in between. Indeed, many authors support the occurrence of a suture zone between the Provence region and the Sardinia-Corsica block, whose remnants are presently underneath the Provence crust (e.g. Lacombe and Jolivet, 2005; Bestani et al., 2016). For the Early to mid-Cretaceous deformation history of Sardinia and Corsica, the only available datum is represented by the work of Mameli et al., (2007) and is illustrated in figure 7b. However, the structure described by these authors for the Sardinia-Corsica block, together with data from the South Provence basin, the Vocontian basin, and the Marguareis system, all point to an Early to mid- Cretaceous N-S to NE-SW directed extension. The N-S to NE-SW extension direction is consistent with the extensional structures of the Pyrenean arm and rules out the hypothesis of a North Pyrenean Fault-Valais strike-slip system. In such a strike-slip system, the Valais dilation jog should open to accommodate the left-lateral motion of Iberia along the North Pyrenean Fault. As a result, the extension direction in the Valais ocean should have formed an angle from 0° to 45° (e.g. Sylvester, 1988) with the plate boundary. Conversely, we have documented in this work that extension was almost perpendicular to the plate boundary, making the strike-slip scenario not supported by geological data and hence, not kinematically admissible. In addition, the idea that Pyrenean rift basins could have developed as pull apart structures that eventually became linked is to be discarded for the following arguments. The hyperextended domain of the eastern Pyrenees, the South Provence basin, the Vocontian basin, and the Marguareis structure form a gross left-stepping system, but not consistent with left-lateral strike-slip tectonics. Data presented in our work indicates that, if any, the hyperextended domain between the Sardinia-Corsica block and the South Provence basin was WNW-ESE elongated and represented the eastern prolongation of the Pyrenean arm. In conclusion, data to the east of the Pyrenees indicate that a plate boundary extended westward from

33

1948
1949
1950
1951
1952
1953
1954
1955
1956
1957
1958
1959
1960
1961
1962
1963
1964
1965
1966
1967
1968
1969
1970
1971
1972
1973
1974
1975
1976
1977
1978
1979
1980
1981
1982
1983
1984
1985
1986
1987
1988
1989
1990
1991
1992
1993
1994
1995
1996
1997
1998
1999
2000
2001
2002
2003
2004
2005
2006

the Bay of Biscay to the Briançonnais domain to the east and had a purely divergent movement during the Early to mid-Cretaceous time interval. In agreement with the lateral evolution of magma-poor rifting (Manatschal, 2004), the Bay of Biscay floored by oceanic crust is the more evolved portion of the rift, the Pyrenean arm, where mantle exhumation is documented, is the intermediate stage, whereas the SE France-Marguareis areas form the less evolved portion of the rift system; such arrangement is coherent with an eastward diminishing amount of divergence. For this long list of evidence, the mid-Cretaceous left-lateral transform model for the Iberia-Eurasia margin should be definitively abandoned. This model has been the paradigm, especially among geologists, for explaining the rotation of Iberia for a very long time (e.g. Souquet et al., 1985; Debroas, 1990; Choukroune, 1992; Olivet, 1996). However, after tens of years of field studies, at the best only equivocal and ambiguous arguments support it. A certain variability of the local extension direction has been documented in the various Cretaceous basins of the margin (e.g. Soto et al., 2008; Olivia-Urcia et al., 2011). The extension is mostly arranged in two mutually perpendicular directions, which is a normal behaviour for extensional systems (e.g. Destro, 1995): such complexity cannot be interpreted as strike-slip tectonics if no evidence for strike-slip motion occurs. Also, the evidence for initially isolated basins that become linked and interconnected, cannot be taken by any reason as an evidence of a pull apart origin. The pattern of faults, and in particular the angular relationships among them and their interpretation according to a Riedel's pattern (Riedel, 1929), has been also invoked as an evidence for the left-lateral strike-slip mid-Cretaceous tectonics (e.g. García-Mondéjar, 1996). However: (1) evidence for left-lateral strike slip striations in such Riedel fault pattern has never been reported in the literature, (2) the occurrence of Variscan and Permo-Triassic inheritances, along with the Upper Cretaceous to Cenozoic reactivation of many of these faults, makes the analysis of the angular relationships alone questionable, as its best. In summary, along the Pyrenees no unequivocal evidence for a Cretaceous lithospheric strike-slip system, comparable for size and displacement to the North Anatolian or San Andrea faults, has ever been provided.

    Having demonstrated the incompatibility between the Cretaceous geological record of the

Iberia-Eurasia plate boundary and both the strike-slip and the scissor type models, a major plate

kinematics issue is to be addressed, as introduced at the beginning of this work, magnetic anomalies

showing a diachrony in the opening of the northern Atlantic (e.g. Sibuet et al., 2004; Vissers and

Meijer, 2012) and paleomagnetic data about the rotation of Iberia (e.g. Barnett-Moore et al., 2016),

are apparently at odds with the divergent model proposed here. This is something known for a long

time (Fig. 1): as already pointed out by Choukroune et al. (1973), if a rigid plate behaviour is

assumed for the Iberia plate, in order to form the Bay of Biscay with coeval extension in the

Pyrenees, the divergent scenario requires an Euler pole to the east of the rift's termination, i.e. to the

east of the Briançonnais Domain. Such pole would be able to account for less than 10° of rotation,

instead of the documented > 30° counter-clockwise rotation (Barnett-Moore et al., 2016, and

references therein). In our view, the key to resolve this apparent discrepancy is the wrong

assumption of a rigid behaviour for the Iberian plate during the Cretaceous divergence, which is all

but certain as it is generally assumed for the sake of simplicity. The importance of intraplate

structures during the separation between Iberia and Eurasia has been recently recalled by Tugend et

al. (2015) but Late Jurassic to Early Cretaceous extension – coeval with the opening of the Bay of

Biscay - focused along the NW-SE striking intra-plate Central Iberian rift is known for a long time

(e.g. Álvaro et al., 1979; Salas and Casas, 1993; Salas et al. 2001). In the Central Iberian rift system,

no mantle exhumation has been reported but evidence for Late Jurassic to mid-Cretaceous extreme

crustal thinning has been provided in its three large depocentres (Fig. 17): the Cameros basin to the

NW (Mata et al., 2001; Salas et al., 2001; Omodeo-Salé et al., 2017), the Maestrat basin to the SE

(e.g. Salas et al., 2001), and the offshore Columbretes basin further to the SE (e.g. Ayala et al.,

2003), where Granado et al. (2016) have even provided evidence for hyper-thinning of the lower

crust and associated mantle faulting. Remarkable extensional deformation, reaching the hyper-

thinning and mantle faulting, implies that the Central Iberian rift could have partially decoupled the

Ebro Block to the NE from the western Iberia to the west (Fig. 17b). Indeed, these two blocks have

a similar amount of Cretaceous counter-clockwise vertical axis rotation but there is no geological

2066
2067
2068
2069
2070
2071
2072
2073
2074
2075
2076
2077
2078
2079
2080
2081
2082
2083
2084
2085
2086
2087
2088
2089
2090
2091
2092
2093
2094
2095
2096
2097
2098
2099
2100
2101
2102
2103
2104
2105
2106
2107
2108
2109
2110
2111
2112
2113
2114
2115
2116
2117
2118
2119
2120
2121
2122
2123
2124

reason, at present, for assuming that these formed a unique rigid block rotating around a unique Eulerian pole. Such partial decoupling of the Ebro block is in line with the observation that in non-oceanic frameworks plates may not behave as rigid objects (Molnar, 1988). This fully applies to the Bay of Biscay-Pyrenean rift system, which displays an increasingly de-localised nature toward its eastern - non-oceanic - termination (Fig. 17b): as said, to the east of the Basque-Cantabrian basin, where no oceanic crust occurs, the rift system splits along two arms: the Pyrenean Arm and the Central Iberian rift, with the Ebro block in between. Further towards its eastern termination, the number of basins progressively increases to the east of the Cévennes transfer fault, where the area undergoing extension reaches a width comparable to that of the entire Iberian plate. In conclusion, if the eastern portion of the Bay of Biscay – Pyrenean rift is considered as a diffuse divergent plate boundary, geological and geophysical observations can be reconciled: the first one indicating extension along the entire length of the rift system during the Early Cretaceous; the second allowing to model the bulk of the movement of the western portion of the Iberian plate by means of counter-clockwise rotation about a pole most likely located in the eastern portion of the Pyrenees.


**6. Conclusions**

In this work we have presented a throughout revision of geological data in the Cretaceous basins to the east of the Pyrenees, in the area comprised between the easternmost portions of the Pyrenees and the Western Alps. Our work evidences that, from the Late Jurassic to the mid-Cretaceous times, the Pyrenean Arm of the rift was undergoing NNE-SSW-directed extension and it was delimited to the east by the NNE-SSW striking Cévennes fault. To the east of this transfer fault, synrift Late Jurassic to mid-Cretaceous N-S extension is documented in the three major E-W elongated extensional basins forming the SE France Arm of the rift system: the Vocontian and South Provence basins, presently exposed in the north-verging portion of the Provence fold-and-thrust belt, and the Figueres-Montgrí basin, which is partly exposed in the easternmost sector of the south-verging portion of the Pyrenees fold-and-thrust belt. In between these basins, an E-W elongated

domain of hyperextended continental crust can be hypothesised. To the east of the SE France Arm, evidence of an even easternmost arm of the rift – i.e. the Briançonnais Arm - occurs in the Marguareis extensional system of the Western Alps. This extensional system holds evidence of N-S extension and it was delimited to the west by a N-S striking transfer fault.

We conclude that the SE France and Briançonnais arms share the same timing and direction of extension with those documented in the Bay of Biscay - Pyrenean rift. Reviewed data along with that presented in this study constrain the Early to mid-Cretaceous divergent movements in the easternmost portion of the of Iberia-Eurasia plate boundary, and support a purely divergent kinematics for the entire plate boundary.

**Figure 1**

Kinematic models proposed in the early 70's to explain the opening of the Bay of Biscay. The motion of Iberia with respect to fixed Eurasia is described by its rigid rotation about a Euler's pole located: (A) to the east of Iberia, (B) near Paris, (C) in the Pyrenean mountain range. Modified from Choukroune et al. (1973)

**Figure 2**

Reconstructions of the Iberia-Eurasia margin and surrounding regions at the mid-Cretaceous time. (A) Rift-perpendicular scenario, after Manatschal and Müntener (2009). (B) Strike-slip scenario, after Stampfli and Borel (2002). (C) Scissor scenario, after Advokaat et al., (2014).

**Figure 3**

Tectonic map of the westernmost Europe, with Late Cretaceous - Cenozoic belts and basins (A), and Mesozoic domains (B), with focus on the architecture of the Bay of Biscay – Pyrenean rift system. The distribution of Mesozoic domains is modified after Tugend et al. (2015) for the Bay of Biscay-Pyrenean area, and from Handy et al., (2010) for the Alps-Apennines area. The position of the Corsica-Sardinia block before the opening of the Liguro-Provençal basin is from Bache et al., (2010). (C) Reconstruction of the Iberia-Eurasia margin and surrounding domains in the mid-Cretaceous, modified from Manatschal and Müntener (2009)

**Figure 4**

Cretaceous extensional structures in the Pyrenean Arm. (A) Detail of the map in figure 3b in the Pyrenean area, with orientation of Cretaceous extension indicated. (B) Table illustrating the timing of major events and the direction of extensional structures in the different domains of the Pyrenean Arm and surrounding areas. References cited in the text and/or indicated in the figure are: Tugend

et al. (2014) for the age of the oceanic crust in the Bay of Biscay. Thinon et al. (2003) and Roca et al. (2011) for the age of mantle exhumation in the Bay of Biscay. Ferrer et al. (2008) for the age of extension and hyperextension in the Parentis basin. García-Mondéjar et al. (1986) and Rat (1988) for the age of extension in the Basque-Cantabrian basin. Biteau et al. (2006) for the age of extension in the Arzacq basin. Jammes et al. (2009), Lagabrielle et al. (2010), and Masini et al. (2014) for the age of hyperextension and mantle exhumation in the Mauléon basin. Souquet et al. (1985) and Debroas (1990) for the age of extension and hyperextension in the Flysch Noir basin. Dinarès-Turell and García-Senz (2000) and García-Senz (2002) for the age of extension in the Organyà basin. Granado et al. (In press) for the extension direction (meso-structural data) in the Asturian basin (indicated as site 1). Soto et al. (2008) and Oliva-Urcia et al. (2013) (AMS data), and Tavani and Muñoz (2012) (meso- and macro-structural data) for the extension direction in the Basque-Cantabrian basin (indicated as site 2). Soto et al. (2008) and García-Lasanta et al. (2014) (AMS), and Mata et al. (2001) (meso-structural data) for the extension direction in the Cameros basin (indicated as site 3). Lagabrielle et al. (2010) for the extension direction (meso-structural data) in the Mauléon extensional detachment (indicated as site 4). Salardon et al. (2017) (meso-structural data) and Olivia-Urcia et al. (2010) (AMS) for the extension direction in the Mauléon basin (indicated as site 5). Passchier (1984) and de Saint Blanquat et al. (1986 and 1990) for the extension direction (meso-structural data) in the Saint Barthélémy massif extensional detachment (indicated as site 6). Vauchez et al. (2013) for the extension direction (meso-structural data) in the Agly massif extensional detachment (indicated as site 7). Gong et al. (2009) and Oliva-Urcia et al. (2011) (AMS data), and Tavani et al. (2011) (meso- and macro-structural data) for the extension direction in the Organyà basin (indicated as site 8).

**Figure 5**

(A) Geological map of the eastern Pyrenees. (B) Cross section across the Bas Agly syncline (after Vauchez et al., 2013). (C) Cross section across the Meda Islands of the Montgrí area (after Mató et

al., 1995b). (D) Geological map of the Figueres area.

**Figure 6**

(A) Detail of the map in figure 3b, showing the location of the Late Jurassic - Cretaceous extensional structures developed on the European margin of the Alpine Tethys, and presently exposed in the Western Alps, in the Languedoc-Provence region of the Pyrenean System, and in Sardinia (B) Facies distribution in the SE France basin, from Triassic to mid-Cretaceous (after Curnelle and Dubois, 1986). (C) Simplified Early Cretaceous structural scheme of the SE France basin, with major faults indicated (after de Graciansky and Lemoine, 1988).

**Figure 7**

(A) Schematic cross-section of the southern margin of the South Provence basin (after Philip et al. (1987). (B) Cross-section of the Olmedo area in Sardinia (after Mameli et al., 2007).

**Figure 8**

Cretaceous extensional structures in eastern Pyrenees and SE France basin. (A) Detail of the map in figure 3b in the area, with orientation of Cretaceous extension indicated. (B) Table illustrating the timing of major events and the direction of extensional structures in the different domains, with data from the Bay of Biscay - Pyrenean Arm in transparency. References cited in the text and/or indicated in the figure are: Saula et al. (1994) and Mató et al. (1995a, 1995b) for the age of extension in the Figueres-Montgrí basin. Guyonnet-Benaize et al. (2010) and Masse et al (2009) for the age of extension in the Vocontian and South Provence basins. Mameli et al. (2007) for the age of extension in the Olmedo area of Sardinia. Mató et al. (1995b) for the extension direction (syn-sedimentary faults orientation) in the Figueres-Montgrí (indicated as site 9). Guyonnet-Benaize et al. (2010), Lamarche et al. (2012), and Homberg et al. (2013) (meso-structures), and de Graciansky and Lemoine (1988) (major faults) for the extension direction in the Vocontian and South Provence

basins (both indicated as site 10). Mameli et al. (2007) (orientation of an extensional fold) for the

extension direction in the Olmedo area of Sardinia (indicated as site 11). Septfontaine (1995) for the

age and direction (orientation of major fault) of extension in the Helvetic domain (indicated as site

12). Cardello and Mancktelow (2014) for the age and direction (meso- and macro-structures) of

extension in the Helvetic domain (indicated as site 13), notice that this could be a gravitational-

structure. Chaulieu (1992), Claudel et al. (1997), and Claudel and Dumont (1999) for the age of

extension in the external Briançonnais Domain of the Western Alps (indicated as site 14).

**Figure 9**

Geological maps of the study area. (A) Map of the Western Alps (modified from d'Atri et al.,

2016), with inset showing the location of figure 9b. The arrows indicate counter-clockwise rotations

about vertical axes (from Collombet et al., 2002). (B) Map of the Marguareis area, with structural

scheme

**Figure 10**

Limone-Viozene northern (LIVZn) Fault in the eastern portion of the study area. (A) Panoramic

view, from the west, of the LIVZn Fault, showing south-dipping Permo-Triassic rocks exposed in

the southern block, and Triassic to Jurassic carbonates of the northern block, faulted by the Passo

delle Saline Fault. (B) Orthophoto with structural scheme of the area and location of photographs

and E-W and N-S oriented geological cross-sections (C) Panoramic view of the northern block of

the LIVZn Fault: W-dipping Triassic and Jurassic carbonates are in the hanging wall of the E-

Dipping Passo delle Saline Fault, which abut onto the LIVZn Fault. (D) Principal displacement

zone of the LIVZn Fault, with Permian Volcanites and Triassic dolostones in the southern and

northern block, respectively. (E) Detail of the fault, showing calcite slicken-fibers indicating a left-

lateral kinematics.

41

**Figure 11**

Details of the Limone-Viozene northern (LIVZn) Fault in the western portion of the study area. (A) View from the north of the fault (for location of the photograph see Fig. 11b), with inset photograph showing a NW-SE striking normal fault in the southern block of the fault. (B) Orthophoto with structural scheme of the area and location of photographs. (C) and (D) E-W striking faults palaeoescarpment in Jurassic carbonates covered by patches of mid-Cretaceous sediments.


**Figure 12**

(A) Orthophoto with structural scheme of the Passo delle Saline Fault area, showing hundreds of metres long N-S striking extensional faults. (B) N-S striking veins affecting Jurassic carbonates


**Figure 13**

(A) Orthophoto with structural scheme of the Colle del Pas Fault area. (B) View from the south of the fault, with W-dipping Permo-Triassic rocks in the footwall and sub-horizontal to slightly W-dipping Upper Cretaceous and Cenozoic rocks in the hanging wall. (C) Detail of the fault showing Permian volcanites underlying a 5-m thick breccia, which in turn is onlapped by Upper Cretaceous marls of the Upega Fm. (D) Three-dimensional virtual outcrop model of the lower portion of the Upega Fm., built by means of multi-view photographs (see Tavani et al., 2016 details). The model is seen in orthographic view along a direction perpendicular to bedding, thus representing a distortion-free properly oriented cross-section of the outcrop, and shows a growth wedge of 15° in the lowermost portion of the Upega Fm.


**Figure 14**

Photograph of Colle del Pas Fault plane as seen in the Piaggia Bella Karstic system


**Figure 15**

42

E-W and N-S oriented cross-sections across the Marguareis extensional system. See text for details.

**Figure 16**

3D scheme illustrating the geometry of the Marguareis Extensional System at early Late Cretaceous.

**Figure 17**

(A) Table illustrating the timing of major events and the direction of extensional structures in the different domains of the study area. (B) Reconstruction of the Iberia-Eurasia margin and surrounding areas in the mid-Cretaceous times, with major basins, transform faults, and crustal domains indicated.

**REFERENCES**

Advokaat, E. L., van Hinsbergen, D. J., Maffione, M., Langereis, C. G., Vissers, R. L., Cherchi, A., Schroeder, R., Madani, H., Columbu, S. (2014). Eocene rotation of Sardinia, and the paleogeography of the western Mediterranean region. Earth and Planetary Science Letters, 401, 183-195.

Alvarez, W., Cocozza, T., Wezel, F.C., 1974. Fragmentation of the Alpine orogenic belt by microplate dispersal. *Nature,* 248, 309-314.

Álvaro, M., Capote, R., Vegas, R. (1979). Un modelo de evolución geotectónica para la Cadena Celtibérica. Acta Geológica Hispánica, 14, 172-177.

Ayala, C., Torné, M., Pous, J. (2003). The lithosphere-asthenosphere boundary in the western Mediterranean from 3D joint gravity and geoid modelling: tectonic implications. Earth and Planetary Science Letters, 209, 275-290

Bache, F., J. L. Olivet, C. Gorini, D. Aslanian, C. Labails, and M. Rabineau (2010), Evolution of rifted continental margins: The case of the Gulf of Lions (Western Mediterranean Basin), *Earth Planet. Sci. Lett.*, *292*(3–4), 345–356, doi:10.1016/j.epsl.2010.02.001.

Barbarand, J., Lucazeau, F., Pagel, M., Séranne, M. (2001). Burial and exhumation history of the south-eastern Massif Central (France) constrained by apatite fission-track thermochronology. Tectonophysics, 335, 275-290.

Barnett-Moore, N., M. Hosseinpour, and S. Maus (2016), Assessing discrepancies between previous plate kinematic models of Mesozoic Iberia and their constraints, *Tectonics, 35*, 1–20, doi:10.1002/(ISSN)1944-9194.

Beltrando, M., D. Rubatto, R. Compagnoni, G. Lister (2007), Was the Valaisian basin floored by oceanic crust? Evidence of Permian magmatism in the Versoyen unit (Valaisian domain, NW Alps), *Ofioliti*, *32*, 85-99.

Beltrando, M., G. Frasca, R. Compagnoni, and A. Vitale-Brovarone (2012), The Valaisan controversy revisited: Multi-stage folding of a Mesozoic hyper-extended margin in the Petit

St. Bernard pass area (Western Alps), *Tectonophysics*, *579*, 17–36, doi:10.1016/j.tecto.2012.02.010.

Bertok, C., L. Martire, E. Perotti, A. D'Atri, and F. Piana (2011), Middle-Late Jurassic syndepositional tectonics recorded in the Ligurian Briançonnais succession (Marguareis–Mongioie area, Ligurian Alps, NW Italy), *Swiss J. Geosci.*, *104*(2), 237–255, doi:10.1007/s00015-011-0058-0.

Bertok, C., L. Martire, E. Perotti, A. D'Atri, and F. Piana (2012), Kilometre-scale palaeoescarpments as evidence for Cretaceous synsedimentary tectonics in the External Briançonnais Domain (Ligurian Alps, Italy), *Sediment. Geol.*, *251–252*, 58–75, doi:10.1016/j.sedgeo.2012.01.012.

Bertok, C., Musso, A., d'Atri, A., Martire, L., Piana, F. (In press). Geology of the Colle di Tenda – Monte Marguareis area (Ligurian Alps, NW Italy). Journal of Maps. doi:10.1080/17445647.2018.1500497

Bestani, L., N. Espurt, J. Lamarche, O. Bellier, and F. Hollender (2016), Reconstruction of the Provence Chain evolution, southeastern France, *Tectonics*, *35*(6), 1506–1525, doi:10.1002/2016TC004115.

Biteau, J. J., Le Marrec, A., Le Vot, M., Masset, J. M. (2006). The Aquitaine Basin. Petroleum Geoscience, 12, 247-273.

Boillot, G., Dupeuble, P.A. & Malod, J. (1979) Subduction and tectonics on the continental margin off northern Spain. Mar. Geol., 32, 53–70.

Bott, M. H. P. (1981). Crustal doming and the mechanism of continental rifting. *Tectonophysics*, *73*(1-3), 1-8.

Bousquet, R., R. Oberhänsli, B. Goffé, M. Wiederkehr, F. Koller, S. M. Schmid, R. Schuster, M. Engi, A. Berger, and G. Martinotti (2008), Metamorphism of metasediments at the scale of an orogen: a key to the Tertiary geodynamic evolution of the Alps*, *Geol. Soc. London, Spec. Publ.*, *298*(1), 393–411, doi:10.1144/SP298.18.

45

Bussy, M.H., M. Eichenberger, N. Giroud, C. Meilhac, S. Presniakov (2008), Early Carboniferous age of the Versoyen ophiolites and consequences: non-existence of a "Valais ocean" (Lower Penninic, western Alps), *Bulletin de la Société Géologique de France*, *179*, 337-355.

Cadenas, P., & Fernández-Viejo, G. (2017). The Asturian Basin within the North Iberian margin (Bay of Biscay): seismic characterization of its geometry and its Mesozoic and Cenozoic cover. *Basin Research*.

Cámara, P. (1997), The Basque-Cantabrian basin's Mesozoic tectono-sedimentary evolution, *Mémoires la Société Géologique Fr.*, *171*, 187–191.

Cardello, G.L., Mancktelow, N.S. (2014). Cretaceous syn-sedimentary faulting in the Wildhorn Nappe (SW Switzerland). Swiss Journal of Geosciences, 107, 223-250.

Carminati, E., M. Lustrino, and C. Doglioni (2012), Geodynamic evolution of the central and western Mediterranean: Tectonics vs. igneous petrology constraints, *Tectonophysics*, *579*, 173–192, doi:10.1016/j.tecto.2012.01.026.

Chaulieu, P. *La sédimentation détritique sur la marge nord-téthysienne témoin de l'évolution géodynamique des Alpes occidentales*. PhD thesis, Université Joseph-Fourier - Grenoble I, 1992.

Choukroune, P., Le Pichon, X., Seguret, M., Sibuet, J. C. (1973). Bay of Biscay and Pyrenees. *Earth and Planetary Science Letters*, *18*, 109-118.

Choukroune P. (1992). Tectonic evolution of the Pyrenees. *Ann. Rev. Earth planet. Sci.,* 20, 143-158

Claudel, M. E., Dumont, T., & Tricart, P. (1997). Une preuve d'extension contemporaine de l'expansion océanique de la Téthys ligure en Briançonnais: les failles du Vallon Laugier. *Comptes Rendus de l'Académie des Sciences-Series IIA-Earth and Planetary Science*, *325*(4), 273-279.

Claudel, M., and Dumont, T., (1999). A record of multistage continental break-up on the Briançonnais marginal plateau (Western Alps): Early and Middle-Late Jurassic rifting.

46

*Eclogae Geologicae Helvetiae*, *92*(1), 45-61.

Clerc, C., Lagabrielle, Y. (2014). Thermal control on the modes of crustal thinning leading to mantle exhumation: Insights from the Cretaceous Pyrenean hot paleomargins. Tectonics, 33, 1340-1359.

Clerc, C., A. Lahfid, P. Monié, Y. Lagabrielle, C. Chopin, M. Poujol, P. Boulvais, J.-C. Ringenbach, E. Masini, and M. de St Blanquat (2015), High-temperature metamorphism during extreme thinning of the continental crust: a reappraisal of the North Pyrenean passive paleomargin, Solid Earth, 6(2), 643–668, doi:10.5194/se-6-643-2015.

Clerc, C., Lagabrielle, Y., Labaume, P., Ringenbach, J. C., Vauchez, A., Nalpas, T., Bousquet R., Ballard J.F., Lahfid A., Fourcade, S. (2016). Basement–Cover decoupling and progressive exhumation of metamorphic sediments at hot rifted margin. Insights from the Northeastern Pyrenean analog. Tectonophysics, 686, 82-97.

Collombet, M., J. C. Thomas, A. Chauvin, P. Tricart, J. P. Bouillin, and J. P. Gratier (2002), Counterclockwise rotation of the western Alps since the Oligocene: New insights from paleomagnetic data, *Tectonics*, *21*(4), 14-1-14–15, doi:10.1029/2001TC901016.

Cotillon, P. 1968. Le Crétacé Inférieur De L'arc Subalpin De Castellane Entre L'asse Et Le Var: Stratigraphie Et Sédimentologie. PhD Thesis, University of Lyon

Coward, M., and D. Dietrich (1989), Alpine tectonics - an overview, *Geol. Soc. London, Spec. Publ.*, *45*(1), 1–29, doi:10.1144/GSL.SP.1989.045.01.01.

Cowie, P.A., Scholz, C.H. (1992). Growth of faults by accumulation of seismic slip. Journal of Geophysical Research 97, 11085-11095.

Curnelle, R., Dubois, P. (1986). Évolution mésozoique des grands bassins sédimentaires Français; bassins de Paris, d'Aquitaine et du Sud-Est. Bulletin de la Société Géologique de France, 2, 529-546.

d'Atri, A., F. Piana, L. Barale, C. Bertok, and L. Martire (2016), Geological setting of the southern

termination of Western Alps, *Int. J. Earth Sci.*, *105*(6), 1831–1858, doi:10.1007/s00531-015-1277-9.

Daignières, M., Séguret, M., Specht, M., and the ECORS Team. (1994). The Arzacq-western Pyrenees ECORS deep seismic profile. In Hydrocarbon and petroleum geology of France, pp. 199-208, Springer Berlin Heidelberg.

De Graciansky, P.-C., R. Busnardo, R. Doublet, and J. Martinod (1987) Tectogenese distensive d'age cretace inferieur aux confins des Baronnies (Chaines subalpines meridionales); liaison avec le rifting atlantique; consequences sur la tectonique alpine, Bulletin de la Société géologique de France, 3, 1211-1214.

De Graciansky, P.-C. Lemoine M., 1988. Early Cretaceous extensional tectonics in the southwestern French Alps: a consequence of North-Atlantic rifting during Tethyan spreading. Bulletin de la Société géologique de France, 4, 733-737.

de Saint Blanquat, M., Brunel, M., Mattauer, M. (1986). Les zones de cisaillements du massif nord Pyrénéen du Saint-Bartelemy, témoins probables del'extension crustale d'âge crétacé. Académie des Sciences, Comptes Rendus, 303, 1339-1344.

de Saint Blanquat, M., Lardeaux, J.M., Brunel, M. (1990). Petrological arguments for high temperature extensional deformation in the Pyrenean Variscan crust (Saint Barthélémy massif, Ariège, France), Tectonophysics, 177, 245-262.

Debroas, E. J. (1990), Le flysch noir albo-cénomanien témoin de la structuration albienne à sénonienne de la zone nord-Pyrénéenne en Bigorre (Hautes Pyrénées, France), Bulletin de la Société géologique de France, 6, 273–286.

Dercourt, J. et al. (1986), Geological evolution of the tethys belt from the atlantic to the pamirs since the LIAS, *Tectonophysics*, *123*(1–4), 241–315, doi:10.1016/0040-1951(86)90199-X.

Destro, N. (1995). Release fault: A variety of cross fault in linked extensional fault systems, in the Sergipe-Alagoas Basin, NE Brazil. Journal of Structural Geology, 17, 615-629.

Deville, E., Mascle, A., Lamiraux, C., Le Bras, A., 1994. Tectonic styles, re-evaluation of plays in

southeastern France. Oil Gas Journal. 92, 53-58

Dewey, J. F., M. L. Helman, S. D. Knott, E. Turco, and D. H. W. Hutton (1989), Kinematics of the western Mediterranean, *Geol. Soc. London, Spec. Publ.*, *45*(1), 265–283, doi:10.1144/GSL.SP.1989.045.01.15.

Dinarès-Turell, J., Garcia-Senz, J. (2000). Remagnetization of Lower Cretaceous limestones from the southern Pyrenees and relation to the Iberian plate geodynamic evolution. Journal of Geophysical Research: Solid Earth, 105, 19405-19418.

Doglioni, C., E. Gueguen, F. Sàbat, and M. Fernandez (1997), The Western Mediterranean extensional basins and the Alpine orogen, *Terra Nov.*, *9*(3), 109–112, doi:10.1046/j.1365-3121.1997.d01-18.x.

Dumont, T., T. Simon-Labric, C. Authemayou, and T. Heymes (2011), Lateral termination of the north-directed Alpine orogeny and onset of westward escape in the Western Alpine arc: Structural and sedimentary evidence from the external zone, *Tectonics*, *30*(5), n/a-n/a, doi:10.1029/2010TC002836.

Dumont, T., S. Schwartz, S. Guillot, T. Simon-Labric, P. Tricart, and S. Jourdan (2012), Structural and sedimentary records of the Oligocene revolution in the Western Alpine arc, *J. Geodyn.*, *56–57*, 18–38, doi:10.1016/j.jog.2011.11.006.

Ellenberger, F. 1967. Les interférences de l'érosion et de la tectonique tangentielle tertiaire dans le Bas-Languedoc (principalement dans l'arc de Saint-Chinian). Note sur les charriages cisaillants, Rev. Géogr. phys. Géol. dyn., 9, 87-142

Faccenna, C. et al. (2014), Mantle dynamics in the Mediterranean, *Rev. Geophys.*, *52*(3), 283–332, doi:10.1002/2013RG000444.

Falvey, D.A. (1974). The development of continental margins in plate tectonic theory. Journal of the Australian Petroleum Exploration Association, 14, 95-106.

Faulds, J.E., Varga, R.J. (1998). The role of accommodation zones and transfer zones in the regional segmentation of extended terranes. Geological Society of America Special Papers,

323, 1-46.

Ferrer, O., Roca, E., Benjumea, B., Muñoz, J. A., Ellouz, N., & MARCONI Team. (2008). The deep seismic reflection MARCONI-3 profile: Role of extensional Mesozoic structure during the Pyrenean contractional deformation at the eastern part of the Bay of Biscay. Marine and Petroleum Geology, 25, 714-730.

Ford, M., Duchene, S., Gasquet, D., Vanderhaeghe, O. (2006). Two-phase orogenic convergence in the external and internal SW Alps. *J. Geol. Soc. London.*, *163*, 815–826, doi:10.1144/0016-76492005-034.

Fortané, A., Duée, G., Lagabrielle, Y., Coutelle, A. (1986). Lherzolites and the western "Chainons béarnais"(French Pyrenees): Structural and paleogeographical pattern. Tectonophysics, 129, 81-98.

Frizon de Lamotte, D., Raulin, C., Mouchot, N., Wrobel-Daveau, J.-C, Blanpied, C., Ringenbach, J.-C. (2011). The southernmost margin of the Tethys realm during the Mesozoic and Cenozoic: Initial geometry and timing of the inversion processes, Tectonics, 30, TC3002, doi:10.1029/2010TC002691.

Froitzheim, N., D. Plašienka, and R. Schuster (2008), Alpine tectonics of the Alps and Western Carpathians, *Geol. Cent. Eur.*, *2*, 1141–1232.

Fry, N. (1989). Southwestward thrusting and tectonics of the western Alps. Geological Society, London, Special Publications, 45, 83-109.

Galdeano, A., Moreau, M.G., Pozzi, J.P., Berthou, P. Y., Malod, J.A. (1989). New paleomagnetic results from Cretaceous sediments near Lisboa (Portugal) and implications for the rotation of Iberia. Earth and Planetary Science Letters, 92, 95-106.

García-Lasanta, C., Oliva-Urcia, B., Román-Berdiel, T., Casas, A.M., Hirt, A.M. (2014). Understanding the Mesozoic kinematic evolution in the Cameros basin (Iberian Range, NE Spain) from magnetic subfabrics and mesostructures. Journal of Structural Geology, 66, 84-101.

García-Mondéjar, J., Agirrezabala, L.M., Aranburu, A., Fernández-Mendiola, P.A., Gómez-Pérez, I., López-Horgue, M., Rosales, I. (1996). Aptian-Albian tectonic pattern of the Basque-Cantabrian Basin (Northern Spain). Geological Journal, 31, 13-45

García-Mondéjar, J., 1996. Plate reconstruction of the Bay of Biscay. Geology 24, 635-638.

García-Senz, J. (2002). Cuencas extensivas del Cretácico Inferior en los Pirineos centrales. Formación y subsecuente inversión. PhD Thesis, Universitat de Barcelona.

Gattacceca, J., A. Deino, R. Rizzo, D. S. Jones, B. Henry, B. Beaudoin, and F. Vadeboin (2007), Miocene rotation of Sardinia: New paleomagnetic and geochronological constraints and geodynamic implications, *Earth Planet. Sci. Lett.*, *258*(3–4), 359–377, doi:10.1016/j.epsl.2007.02.003.

Gawthorpe, R. L., & Hurst, J. M. (1993). Transfer zones in extensional basins: their structural style and influence on drainage development and stratigraphy. Journal of the Geological Society, 150(6), 1137-1152.

Gibbs, A. D. (1984). Structural evolution of extensional basin margins. *Journal of the Geological Society*, *141*(4), 609-620.

Goffé, B., and C. Chopin (1986), High-pressure metamorphism in the Western Alps: zoneography of metapelites, chronology and consequences, *Schweizerische Mineral. und Petrogr. Mitteilungen*, *66*(1–2), 41–52.

Gong, Z., Langereis, C.G., Mullender, T.A.T. (2008). The rotation of Iberia during the Aptian and the opening of the Bay of Biscay. Earth and Planetary Science Letters, 273, 80-93.

Gong, Z., Van Hinsbergen, D.J.J., Vissers, R.L.M., Dekkers, M.J. (2009). Early Cretaceous syn-rotational extension in the Organyà basin--New constraints on the palinspastic position of Iberia during its rotation. Tectonophysics, 473, 312-323.

Granado, P., Urgeles, R., Sàbat, F., Albert-Villanueva, E., Roca, E., Muñoz, J.A., Mazzucca N., Gambini, R. (2016). Geodynamical framework and hydrocarbon plays of a salt giant: the NW Mediterranean Basin. Petroleum Geoscience, 22, 309-321.

Granado, P., Tavani, S., Carrera, N., Muñoz, J.A. (In Press). Deformation pattern around the Conejera Fault blocks (Asturian Basin, North Iberian Margin). Geologica Acta.

Guyonnet-Benaize, C., Lamarche, J., Masse, J.P., Villeneuve, M., Viseur, S. (2010). 3D structural modelling of small-deformations in poly-phase faults pattern. Application to the Mid-Cretaceous Durance uplift, Provence (SE France). Journal of Geodynamics, 50, 81-93.

Handy, M. R., S. M. Schmid, R. Bousquet, E. Kissling, and D. Bernoulli (2010), Reconciling plate-tectonic reconstructions of Alpine Tethys with the geological–geophysical record of spreading and subduction in the Alps, *Earth-Science Reviews*, *102*, 121–158, doi:10.1016/j.earscirev.2010.06.002.

Hennuy, J. (2003) - Sédimentation carbonatée et silicoclastique sous contrôle tectonique, le bassin Sud-Provençal et sa plate-forme carbonatée au Turonien moyen au Coniacien moyen. Evolutions séquentielle, diagénétique, paleogéographique. Thèse de Doctorat de l'Université de Provence, Marseille, 252 p.

Hibsch, C., D. Kandel, C. Montenat, and P. O. d'Estevou (1992), Evenements tectoniques cretaces dans la partie meridionale du bassin subalpin (massif Ventoux-Lure et partie orientale de l'arc de Castellane, SE France); implications geodynamiques, *Bull. la Soc. Geol. Fr.*, *163*(2), 147–158.

Hippolyte, J.-C., J. Angelier, F. Bergerat, D. Nury, and G. Guieu (1993), Tectonic-stratigraphic record of paleostress time changes in the Oligocene basins of the Provence, southern France, *Tectonophysics*, *226*(1–4), 15–35, doi:10.1016/0040-1951(93)90108-V.

Homberg, C., J. Schnyder, and M. Benzaggagh (2013), Late Jurassic-Early Cretaceous faulting in the Southeastern French basin: does it reflect a tectonic reorganization?, *Bull. la Soc. Geol. Fr.*, *184*(4–5), 501–514, doi:10.2113/gssgfbull.184.4-5.501.

Huismans, R. S., Podladchikov, Y.Y., Cloetingh, S. (2001). Transition from passive to active rifting: Relative importance of asthenospheric doming and passive extension of the lithosphere. Journal of Geophysical Research: Solid Earth, 106, 11271-11291.

Huismans, R., Beaumont, C. (2011). Depth-dependent extension, two-stage breakup and cratonic underplating at rifted margins. Nature, 473, 74-78.

Jammes, S., G. Manatschal, L. Lavier, and E. Masini (2009), Tectonosedimentary evolution related to extreme crustal thinning ahead of a propagating ocean: Example of the western Pyrenees, *Tectonics*, *28*(4), n/a-n/a, doi:10.1029/2008TC002406.

Jammes, S., Lavier, L., Manatschal, G. (2010). Extreme crustal thinning in the Bay of Biscay and the Western Pyrenees: From observations to modeling. Geochemistry, Geophysics, Geosystems, 11, DOI: 10.1029/2010GC003218

Johnson, J. A., and C. A. Hall (1989), Tectono-stratigraphic model for the Massif D'Igountze-Mendibelza, western Pyrenees, *J. Geol. Soc. London.*, *146*(6), 925–932, doi:10.1144/gsjgs.146.6.0925.

Jolivet, L., C. Gorini, J. Smit, and S. Leroy (2015), Continental breakup and the dynamics of rifting in back-arc basins: The Gulf of Lion margin, *Tectonics*, *34*(4), 662–679, doi:10.1002/2014TC003570.

Kerckhove, C. (1969), La "zone du Flysch" dans les nappes de l'Embrunais-Ubaye (Alpes occidentales), *Géologie Alp.*, *45*, 5–204.

Kim, Y.S., Sanderson, D.J. (2005). The relationship between displacement and length of faults: a review. Earth-Science Reviews 68, 317-334.

Kooi, H., Cloetingh, S., Burrus, J. (1992). Lithospheric necking and regional isostasy at extensional basins 1. Subsidence and gravity modeling with an application to the Gulf of Lions margin (SE France). Journal of Geophysical Research: Solid Earth, 97, 17553-17571.

Lacombe, O., and L. Jolivet (2005), Structural and kinematic relationships between Corsica and the Pyrenees-Provence domain at the time of the Pyrenean orogeny, *Tectonics*, *24*(1), n/a-n/a, doi:10.1029/2004TC001673.

Lacroix, A. (1895), *Les phénomènes de contact de la lherzolite et de quelques ophites des Pyrénées*, Librairie polytechnique, Baudry et cie.

Lagabrielle, Y., and J.-L. Bodinier (2008), Submarine reworking of exhumed subcontinental mantle rocks: field evidence from the Lherz peridotites, French Pyrenees, *Terra Nova*, *20*(1), 11–21, doi:10.1111/j.1365-3121.2007.00781.x.

Lagabrielle, Y., Labaume, P., & de Saint Blanquat, M. (2010). Mantle exhumation, crustal denudation, and gravity tectonics during Cretaceous rifting in the Pyrenean realm (SW Europe): Insights from the geological setting of the lherzolite bodies. *Tectonics*, *29*(4).

Lamarche, J., Lavenu, A.P.C., Gauthier, B.D.M., Guglielmi, Y., & Jayet, O. (2012). Relationships between fracture patterns, geodynamics and mechanical stratigraphy in carbonates (South-East Basin, France). *Tectonophysics,* 581, 231–245.

Lanaja, J. M. (1987), *Contribución de la exploración petrolífera al conocimiento de la geología de España*, IGME.

Larrasoaña, J. C., Parés, J. M., Millán, H., Del Valle, J., & Pueyo, E. L. (2003). Paleomagnetic, structural, and stratigraphic constraints on transverse fault kinematics during basin inversion: The Pamplona Fault (Pyrenees, north Spain). *Tectonics*, *22*(6).

Lemoine, 1984; M. Lemoine; La marge occidentale de la Tethys ligure et des Alpes occidentales. G. Boillot (Ed.), Les Marges Continentales Autour de la France, Masson Edition, Paris (1984), pp. 155–182

Lemoine, M., Bas, T., Arnaud-Vanneau, A., Arnaud, H., Dumont, T., Gidon, M., Bourbon, M., de Graciansky, P.-C., Rudkiewicz, J.-L., Megard-Galli, J., Tricart, P. (1986). The continental margin of the Mesozoic Tethys in the Western Alps. *Marine and petroleum geology*, *3*(3), 179-199.

Lemoine, M., P. C. De Graciansky, and P. Tricart (2000), *De l'océan à la chaîne de montagnes: tectonique des plaques dans les Alpes*, Editions scientifiques GB.

Lepvrier, C., Martínez-García, E. (1990). Fault development and stress evolution of the post-Hercynian Asturian Basin (Asturias and Cantabria, northwestern Spain). Tectonophysics, 184, 345-356.

Liati A, Froitzheim N (2006) Assessing the Valais ocean, Western Alps: U-Pb SHRIMP zircon geochronology of eclogite in the Balma unit, on top of the Monte Rosa nappe. Eur J Mineral 18(3):299–308

Lister, G.S., Etheridge, M.A., and Symonds, P.A., 1991, Detachment models for the formation of passive continental margins: Tectonics, v. 10, p. 1038-1064

López-Mir, B., Muñoz, J.A., García-Senz, J. (2015). Extensional salt tectonics in the partially inverted Cotiella post-rift basin (south-central Pyrenees): structure and evolution. International Journal of Earth Sciences, 104, 419-434.

Louis, L., Robion, P., David, C., Frizon de Lamotte, D. (2006). Multiscale anisotropy controlled by folding: the example of the Chaudrons fold (Corbieres, France). Journal of Structural Geology, 28, 549-560.

Malusà, M. G., Faccenna, C., Garzanti, E., Polino, R. (2011). Divergence in subduction zones and exhumation of high pressure rocks (Eocene Western Alps). Earth and Planetary Science Letters, 310, 21-32.

Mata, M.P., Casas, A.M., Canals, A., Gil, A., Pocovi, A. (2001). Thermal history during Mesozoic extension and Tertiary uplift in the Cameros Basin, northern Spain. Basin Research, 13, 91-111.

Mameli, P., Mongelli, G., Oggiano, G., Dinelli, E. (2007). Geological, geochemical and mineralogical features of some bauxite deposits from Nurra (Western Sardinia, Italy): insights on conditions of formation and parental affinity. International Journal of Earth Sciences, 96, 887-902.

Manatschal G, Müntener O. (2009) A type sequence across an ancient magma-poor ocean-continent transition: the example of the western Alpine Tethys ophiolites. Tectonophysics 473(1–2):4–19

Manatschal, G. (2004). New models for evolution of magma-poor rifted margins based on a review of data and concepts from West Iberia and the Alps. International Journal of Earth Sciences,

93, 432-466.

Manatschal, G., Lavier, L., Chenin, P. (2015). The role of inheritance in structuring hyperextended rift systems: Some considerations based on observations and numerical modeling. Gondwana Research, 27, 140-164.

Martire, L., C. Bertok, A. D'atri, E. Perotti, and F. Piana (2014), Selective dolomitization by syntaxial overgrowth around detrital dolomite nuclei: a case from the Jurassic of the Ligurian Briançonnais (Ligurian Alps), *J. Sediment. Res.*, *84*(1), 40–50.

Masini, E., G. Manatschal, J. Tugend, G. Mohn, and J.-M. Flament (2014), The tectono-sedimentary evolution of a hyper-extended rift basin: the example of the Arzacq–Mauléon rift system (Western Pyrenees, SW France), *Int. J. Earth Sci.*, *103*(6), 1569–1596, doi:10.1007/s00531-014-1023-8.

Masse, J. P., and J. Philip. (1976), Paléogéographie et tectonique du Crétacé moyen en Provence: révision du concept d'isthme durancien. *Revue de Géographie physique et de Géologie dynamique,* 18.1, 49-66.

Masse, J. P., Villeneuve, M., Leonforte, E., & Nizou, J. (2009). Block tilting of the North Provence early Cretaceous carbonate margin: stratigraphic, sedimentologic and tectonic data. *Bulletin de la société géologique de France*, *180*(2), 105-115.

Mató, E., Saula, E., Picart, J., Solà, J., Montaner, J., Serra, J., Caus, E. (1995a). Geological map of Catalunya 1:25000. Sheet 296-2-1. Institut Cartogràfic i Geològic de Catalunya. Barcelona.
Mató, E., Saula, E., Montaner, J., Solà, J., Caus, E., Serra, J. (1995b). Geological map of Catalunya 1:25000. Sheet 297-1-2. Institut Cartogràfic i Geològic de Catalunya. Barcelona.

Mauffret, A., and M. Gennesseaux (1989), Compression, décrochements et distension sur le pourtour méditerranéen nord-occidental, *Comptes rendus l'Académie des Sci. Série 2, Mécanique, Phys. Chim. Sci. l'univers, Sci. la Terre*, *308*(10), 961–967.

Mazzoli, S., and M. Helman (1994), Neogene patterns of relative plate motion for Africa-Europe: some implications for recent central Mediterranean tectonics, *Geol. Rundschau*, *83*(2), 464–

468, doi:10.1007/BF00210558.

McKenzie, D. (1978). Some remarks on the development of sedimentary basins. *Earth and Planetary science letters*, *40*(1), 25-32.

Mencos, J., Carrera, N., Muñoz, J.A. (2015). Influence of rift basin geometry on the subsequent postrift sedimentation and basin inversion: The Organyà Basin and the Bóixols thrust sheet (south central Pyrenees). Tectonics, 34, 1452-1474, doi: 10.1002/2014TC003692.

Merle, O. (1982), Mise en place séquentielle de la Nappe du Parapaillon en Embrunais-Ubaye (Flysch à Helminthoïdes, Alpes occidentales), *Comptes Rendus l'Académie des Sci. Paris*, *294*, 603–606.

Michard, A., Martinotti, G., (2002) The Eocene unconformity of the Brianconnais domain in the French-Italian Alps, revisited (Marguareis massif, Cuneo); a hint for a Late Cretaceous-Middle Eocene frontal bulge setting. Geodinamica Acta, 15, 289-301

Michard, A., D. Avigad, B. Goffé, and C. Chopin (2004), The high-pressure metamorphic front of the south Western Alps (Ubaye-Maira transect, France, Italy), *Schweiz. Miner. Petrogr. Mitt*, *84*, 215–235.

Mohn, G., G. Manatschal, O. Müntener, M. Beltrando, and E. Masini (2010), Unravelling the interaction between tectonic and sedimentary processes during lithospheric thinning in the Alpine Tethys margins, *Int. J. Earth Sci.*, *99*(S1), 75–101, doi:10.1007/s00531-010-0566-6.

Molliex, S., O. Bellier, M. Terrier, J. Lamarche, G. Martelet, and N. Espurt (2011), Tectonic and sedimentary inheritance on the structural framework of Provence (SE France): Importance of the Salon-Cavaillon fault, *Tectonophysics*, *501*(1–4), 1–16, doi:10.1016/j.tecto.2010.09.008.

Molnar, P. (1988). Continental tectonics in the aftermath of plate tectonics. Nature, 335, 131-137.

Montenat, C., C. Hibsch, J. C. Perrier, F. Pascaud, and P. de Bretizel (1997), Tectonique cassante d'âge Crétacé inférieur dans l'arc de Nice (Alpes-Maritimes, France), *Géologie Alp.*, *73*, 59–66.

Morley, C. K., Nelson, R. A., Patton, T. L., & Munn, S. G. (1990). Transfer zones in the East African rift system and their relevance to hydrocarbon exploration in rifts (1). *AAPG Bulletin*, *74*(8), 1234-1253.

Mouthereau, F., P.-Y. Filleaudeau, A. Vacherat, R. Pik, O. Lacombe, M. G. Fellin, S. Castelltort, F. Christophoul, and E. Masini (2014), Placing limits to shortening evolution in the Pyrenees: Role of margin architecture and implications for the Iberia/Europe convergence, *Tectonics*, *33*(12), 2283–2314, doi:10.1002/2014TC003663.

Muñoz, J.A. (1992). Evolution of a continental collision belt: ECORS-Pyrenees crustal balanced cross-section. In: McClay (Ed.), Thrust Tectonics. Chapman & Hall, London, 235-246.

Muñoz, J. A. (2002). The Pyrenees. In: The Geology of Spain, W. Gibbons and M. T. Moreno (eds.), pp. 370-385, Geological Society, London, U. K.

Nirrengarten, M., Manatschal, G., Tugend, J., Kusznir, N.J. Sauter, D. (2017). Nature and origin of the J-magnetic anomaly offshore Iberia–Newfoundland: implications for plate reconstructions. Terra Nova, 29, 20-28.

Neres, M., Font, E., Miranda, J. M., Camps, P., Terrinha, P., Mirão, J. (2012). Reconciling Cretaceous paleomagnetic and marine magnetic data for Iberia: New Iberian paleomagnetic poles. Journal of Geophysical Research: Solid Earth, 117, B06102.

Olivet, J. L. (1996), La cinématique de la plaque ibérique, *Bull. Cent. Rech. Explor. Prod. Elf Aquitaine*, *20*(1), 131–195.

Oliva-Urcia, B., Román-Berdiel, T., Casas, A.M., Pueyo, E.L., Osácar, C. (2010). Tertiary compressional overprint on Aptian-Albian extensional magnetic fabrics, North Pyrenean Zone. Journal of Structural Geology, 32, 362-376

Oliva-Urcia, B., Casas, A.M., Soto, R., Villalaín, J.J., Kodama, K. (2011). A transtensional basin model for the Organyà basin (central southern Pyrenees) based on magnetic fabric and brittle structures. Geophysical Journal International, 184, 111-130.

Oliva-Urcia, B., Román-Berdiel, T., Casas, A.M., Bógalo, M. F., Osácar, M. C., García-Lasanta, C.

(2013). Transition from extensional to compressional magnetic fabrics in the Cretaceous Cabuérniga basin (North Spain). Journal of Structural Geology, 46, 220-234.

Omodeo-Salé, S., Salas, R., Guimerà, J., Ondrak, R., Mas, R., Arribas, J., Suárez-Ruiz, I., Martínez, L. (2017). Subsidence and thermal history of an inverted Late Jurassic-Early Cretaceous extensional basin (Cameros, North-central Spain) affected by very low to low-grade metamorphism. Basin Research, 51, 156-174, doi:10.1111/bre.12142

Passchier, C. W., (1984), Mylonite dominated footwall geometry in a shear zone, central Pyrénées, Geological Magazine, 121, 429-436.

Pedreira, D., Afonso, J. C., Pulgar, J. A., Gallastegui, J., Carballo, A., Fernàndez, M., García-Castellanos, D., Jiménez-Munt, I., Semprich, J. and García-Moreno, O. (2015). Geophysical-petrological modeling of the lithosphere beneath the Cantabrian Mountains and the North-Iberian margin: geodynamic implications, *Lithos*, 230(C), 46–68. http://doi.org/10.1016/j.lithos.2015.04.018

Philip, J. (1970) - Les formations calcaires à rudistes du Crétacé supérieur provençal et rhodanien. Thèse de Doctorat d'Etat, Marseille, 433 p.

Philip, J., Masse, J. L., Machhour, L. (1987). L'evolution paleogeographique et structurale du front de chavauchement nord-toulonnais (Basse-Provence occidentale, France). Bulletin de la Société géologique de France, 3, 541-550.

Pi, E., Solà, J., Montaner, J., Picart, J., Samso, J.M., Calvet, F., Mato, E., Pujades, J., Saula, E., Caus, E. Berastegui, X. (1997). Geological map of Catalunya 1:25000. Sheet 258-1-1. Institut Cartogràfic i Geològic de Catalunya. Barcelona.

Piana, F., A. Musso, C. Bertok, A. D'Atri, L. Martire, E. Perotti, D. Varrone, and G. Martinotti (2009), New data on post-Eocene tectonic evolution of the external Ligurian Briançonnais (Western Ligurian Alps), *Boll. della Soc. Geol. Ital.*, *128*(2), 353–366, doi:10.3301/IJG.2009.128.2.353.

Piana, F., S. Battaglia, C. Bertok, A. D'atri, A. Ellero, L. Leoni, L. Martire, and E. Perotti (2014),

Illite (KI) and chlorite (AI) "crystallinity" indices as a constraint for the evolution of the External Briançonnais Front in Western Ligurian Alps (NW Italy), *Ital. J. Geosci.*, *133*(3), 445–454, doi:10.3301/IJG.2014.21.

Puigdefàbregas, C., Souquet, P. (1986). Tecto-sedimentary cycles and depositional sequences of the Mesozoic and Tertiary from the Pyrenees. Tectonophysics, 129, 173-203.

Pujadas, J., Casas, M. Muñoz, J.A., Sabat, F. (1989). Thrust tectonics and Paleogene syntectonic sedimentation in the Emporda area, southeastern Pyrenees. Geodinamica Acta, 3, 195-206.

Rat, P. (1988), The Basque-Cantabrian basin between the Iberian and European plates: Some facts but still many problems, *Rev. la Soc. geológica España*, *1*(3–4), 327–348.

Rehault, J. P., J. Mascle, and G. Boillot (1984), Evolution géodynamique de la Méditerranée depuis l'Oligocene, *Mem. Soc. Geol. Ital*, *27*, 85–96.

Riedel, W., 1929. Zur mechanik geologischer brucherscheinungen, Zentralblatt für Mineralogie. Geologie und Paläontologie 1929B, 354–368.

Roca, E., J. A. Muñoz, O. Ferrer, and N. Ellouz (2011), The role of the Bay of Biscay Mesozoic extensional structure in the configuration of the Pyrenean orogen: Constraints from the MARCONI deep seismic reflection survey, Tectonics, 30(2), n/a-n/a, doi:10.1029/2010TC002735.

Rosenbaum, G., Lister, G. S. (2005). The Western Alps from the Jurassic to Oligocene: spatio-temporal constraints and evolutionary reconstructions. Earth-Science Reviews, 69(3-4), 281-306.

Roure, F., Choukroune, P., Berastegui, X., Muñoz, J. A., Villien, A., Matheron, P., Bareyt, M., Seguret, M., Camara, P., Deramond, J. (1989). ECORS deep seismic data and balanced cross sections: Geometric constraints on the evolution of the Pyrenees. Tectonics, 8, 41-50, doi: 10.1029/TC008i001p00041

Rouvier, H., Henry, B., Le Goff, M. (2012). Mise en évidence par le paléomagnétisme de rotations régionales dans la virgation des Corbières (France). Bulletin de la Société géologique de

France, 183, 409-424.

Royden, L., Keen, C.E. (1980). Rifting process and thermal evolution of the continental margin of eastern Canada determined from subsidence curves. Earth and Planetary Science Letters, 51, 343-361.

Salardon, R., Carpentier, C., Bellahsen, N., Pironon, J., France-Lanord, C. (2017). Interactions between tectonics and fluid circulations in an inverted hyper-extended basin: Example of mesozoic carbonate rocks of the western North Pyrenean Zone (Chaînons Béarnais, France). Marine and Petroleum Geology, 80, 563-586.

Salas, R., Guimerà, J., Mas, R., Martín-Closas, C., Meléndez, A., Alonso, A. (2001). Evolution of the Mesozoic central Iberian Rift System and its Cainozoic inversion (Iberian chain). In Peri-Tethys memoir, 6: Peri-Tethyan Rift/Wrench Basins and Passive Margins (eds P. A. Ziegler, W. Cavazza, A. H. F. Robertson & S. Crasquin-Soleau), Mémoires de Muséum National d'Histoire Naturelle, 186, 145-186.

Salas, R., Casas, A. (1993). Mesozoic extensional tectonics, stratigraphy and crustal evolution during the Alpine cycle of the eastern Iberian basin. *Tectonophysics*, *228*, 33-55.

Saula, E., Mató, E., Montaner, J., Solà, J., Picart, J., Agustì, J., Lienas, M., Moya, S., Serra, J., Caus, E. (1994). Geological map of Catalunya 1:25000. Sheet 296-2-2. Institut Cartogràfic i Geològic de Catalunya. Barcelona.

Saura, E., Ardèvol i Oró, L., Teixell, A., Vergés, J. (2016). Rising and falling diapirs, shifting depocenters, and flap overturning in the Cretaceous Sopeira and Sant Gervàs subbasins (Ribagorça Basin, southern Pyrenees). Tectonics, 35, 638-662.

Schlunegger, F., Kissling, E. (2015). Slab rollback orogeny in the Alps and evolution of the Swiss Molasse basin. *Nature communications*, *6*, 8605.

Schmid, S. M., Kissling, E. (2000), The arc of the western Alps in the light of geophysical data on deep crustal structure. *Tectonics* 19, 62-85.

Schmid, S. M., O. A. Pfiffner, N. Froitzheim, G. Schönborn, and E. Kissling (1996), Geophysical-

geological transect and tectonic evolution of the Swiss-Italian Alps, *Tectonics*, *15*(5), 1036–1064, doi:10.1029/96TC00433.

Schmid, S. M., B. Fügenschuh, E. Kissling, and R. Schuster (2004), Tectonic map and overall architecture of the Alpine orogen, *Eclogae Geol. Helv.*, *97*(1), 93–117, doi:10.1007/s00015-004-1113-x.

Sengör, A. M., Burke, K. (1978). Relative timing of rifting and volcanism on Earth and its tectonic implications. *Geophysical Research Letters*, *5*, 419-421.

Septfontaine, M., 1995. Large scale progressive unconformities in Jurassic strata of the Prealps S of lake Geneva. Interpretation as synsedimentary inversion structures; paleotectonic implications. Eclogae Geol. Helv. 88, 553–576

Séranne, M. (1999), The Gulf of Lion continental margin (NW Mediterranean) revisited by IBS: an overview, *Geol. Soc. London, Spec. Publ.*, *156*(1), 15–36, doi:10.1144/GSL.SP.1999.156.01.03.

Séranne, M., A. Benedicto, P. Labaum, C. Truffert, and G. Pascal (1995), Structural style and evolution of the Gulf of Lion Oligo-Miocene rifting: role of the Pyrenean orogeny, *Mar. Pet. Geol.*, *12*(8), 809–820, doi:10.1016/0264-8172(95)98849-Z.

Sibuet, J.-C., S. P. Srivastava, and W. Spakman (2004), Pyrenean orogeny and plate kinematics, J. Geophys. Res. Solid Earth, 109(B8), doi:10.1029/2003JB002514.

Souque, C., Robion, P., Frizon de Lamotte, D., 2002. Cryptic magnetic fabric of tectonic origin revealed by heating of sedimentary samples from the Corbières, France. Physics and Chemistry of the Earth, 27, 1253–1262.

Soto, R., Casas-Sainz, A.M., Villalain, J.J., Gil-Imaz, A., Fernández-González, G., Del Río, P., Calvo, M., Mochales, T. (2008). Characterizing the Mesozoic extension direction in the northern Iberian Plate margin by anisotropy of magnetic susceptibility (AMS). Journal of the Geological Society of London 165, 1007-1018.

Souquet P. , Debroas E.-J., Boirie J.-M., Pons P., Fixari G., Dol J., Thieuloy J.-P., Bonnemaison M.,

Manivit H., Peybernès B. (1985). Le groupe du Flysch noir (albo-cénomanien) dans les Pyrénées. Bull. Centres Rech. Explor. Prod. Elf-Aquitaine, 9, 183-252

Stampfli, G. M., Mosar, J., Marquer, D., Marchant, R., Baudin, T., Borel, G. (1998). Subduction and obduction processes in the Swiss Alps. *Tectonophysics*, *296*(1-2), 159-204.

Stampfli, G. M., & Borel, G. D. (2002). A plate tectonic model for the Paleozoic and Mesozoic constrained by dynamic plate boundaries and restored synthetic oceanic isochrons. *Earth and Planetary Science Letters*, *196*(1), 17-33.

Stampfli, G. M., & Hochard, C. (2009). Plate tectonics of the Alpine realm. *Geological Society, London, Special Publications*, *327*(1), 89–111. http://doi.org/10.1144/SP327.6

Sylvester, A. G. (1988). Strike-slip faults. *Geological Society of America Bulletin*, *100*, 1666-1703.

Tassone, A., Roca, E., Muñoz, J.A., Cabrera, L., Canals, M. (1994). Evolución del sector septentrional del margen continental catalán durante el Cenozoico. Acta geológica hispánica, 29, 3-37.

Tavani, S., Mencos, J., Bausà, J., Muñoz, J.A. (2011). The fracture pattern of the Sant Corneli Bóixols oblique inversion anticline (Spanish Pyrenees). Journal of Structural Geology, 33, 1662-1680.

Tavani, S., Muñoz, J.A., (2012). Mesozoic rifting in the Basque–Cantabrian Basin (Spain): inherited faults, transversal structures and stress perturbation. Terra Nova, 24, 70-76.

Tavani, S., and P. Granado (2015), Along-strike evolution of folding, stretching and breaching of supra-salt strata in the Plataforma Burgalesa extensional forced fold system (northern Spain), *Basin Res.*, *27*(4), 573–585, doi:10.1111/bre.12089.

Tchalenko, J. S. (1970), Similarities between Shear Zones of Different Magnitudes, *Geol. Soc. Am. Bull.*, *81*(6), 1625, doi:10.1130/0016-7606(1970)81[1625:SBSZOD]2.0.CO;2.

Teixell, A. (1998). Crustal structure and orogenic material budget in the west central Pyrenees, Tectonics, 17, 395-406, doi:10.1029/98TC00561

Teixell, A., Labaume, P., Lagabrielle, Y. (2016). The crustal evolution of the west-central Pyrenees

revisited: Inferences from a new kinematic scenario. Comptes Rendus Geoscience, 348, 257-267.

Thinon, I., Réhault, J.P., Fidalgo-González, L. (2002). The syn-rift sedimentary cover of the North Biscay Margin (bay of Biscay): From new reflection seismic data. Bulletin de la Société Géologique de France, 173, 515-522.

Thinon, I., Matias, L., Réhault, J.P., Hirn, A., Fidalgo-González, L., Avedik, F. (2003). Deep structure of the Armorican Basin (Bay of Biscay): A review of Norgasis seismic reflection and refraction data. Journal of the Geological Society of London, 160, 99-116.

Thomas, J. C., M. E. Claudel, M. Collombet, P. Tricart, A. Chauvin, and T. Dumont (1999), First paleomagnetic data from the sedimentary cover of the French Penninic Alps: evidence for Tertiary counterclockwise rotations in the Western Alps, *Earth Planet. Sci. Lett.*, *171*(4), 561–574, doi:10.1016/S0012-821X(99)00182-X.

Tugend, J., G. Manatschal, N. J. Kusznir, E. Masini, G. Mohn, and I. Thinon (2014), Formation and deformation of hyperextended rift systems: Insights from rift domain mapping in the Bay of Biscay-Pyrenees, *Tectonics*, *33*(7), 1239–1276, doi:10.1002/2014TC003529.

Tugend, J., Manatschal, G., Kusznir, N. (2015). Spatial and temporal evolution of hyperextended rift systems: Implication for the nature, kinematics, and timing of the Iberian-European plate boundary. Geology, 43, 15-18.

van der Beek, P.A., Cloetingh, S., Andriessen, P.A.M., 1994. Extensional basin formation mechanisms and vertical motion of rift flanks: constraints from tectonic modelling and fission-track thermochronology. Earth Planet. Sci. Lett. 121, 417 – 433.

van der Voo, R. (1969). Paleomagnetic evidence for the rotation of the Iberian Peninsula, Tectonophysics, 7, 5-56.

Vanossi, M. (1969). La serie brianzonese del Salto del Lupo (Liguria occidentale): osservazioni sedimentologico-stratigrafiche. Atti Ist. Geol. Univ. Pavia, 20, 3-16.

Vanossi, M. (1972). Rilevamento geologico ed analisi strutturale delle dorsali del M. Mongioie e

del M. Cimone. Atti Ist. Geol. Univ. Pavia, 23, 29-71.

Vauchez, A., Clerc, C., Bestani, L., Lagabrielle, Y., Chauvet, A., Lahfid, A., Mainprice, D. (2013). Preorogenic exhumation of the North Pyrenean Agly massif (Eastern Pyrenees France). *Tectonics*, *32*(2), 95-106.

Vergés, J., García-Senz, J. (2001). Mesozoic evolution and Cainozoic inversion of the Pyrenean rift. Mémoires du Muséum national d'histoire naturelle, 186, 187-212.

Vergés, J., M. Fernàndez, and A. Martínez (2002), The Pyrenean orogen: pre-, syn-, and post-collisional evolution, *J. Virtual Explor.*, *8*, 57–76.

Vielzeuf, D. and Kornprobst, J. (1984). Crustal splitting and the emplacement of Pyrenean lherzolites and granulites, Earth Planet. Science Lett., 67, 87–96.

Vissers, R. L. M., and P. T. Meijer (2012), Mesozoic rotation of Iberia: Subduction in the Pyrenees?, *Earth-Science Rev.*, *110*(1–4), 93–110, doi:10.1016/j.earscirev.2011.11.001.

Vissers, R. L., van Hinsbergen, D. J., Van Der Meer, D. G., Spakman, W. (2016). Cretaceous slab break-off in the Pyrenees: Iberian plate kinematics in paleomagnetic and mantle reference frames. *Gondwana Research*, *34*, 49-59.

Wilson, J.T., 1965, A new class of faults and their bearing on continental drift, Nature, 207, 343-347.

Ziegler, P.A., Cloetingh, S. (2004). Dynamic processes controlling evolution of rifted basins. Earth-Science Reviews, 64, 1-50.
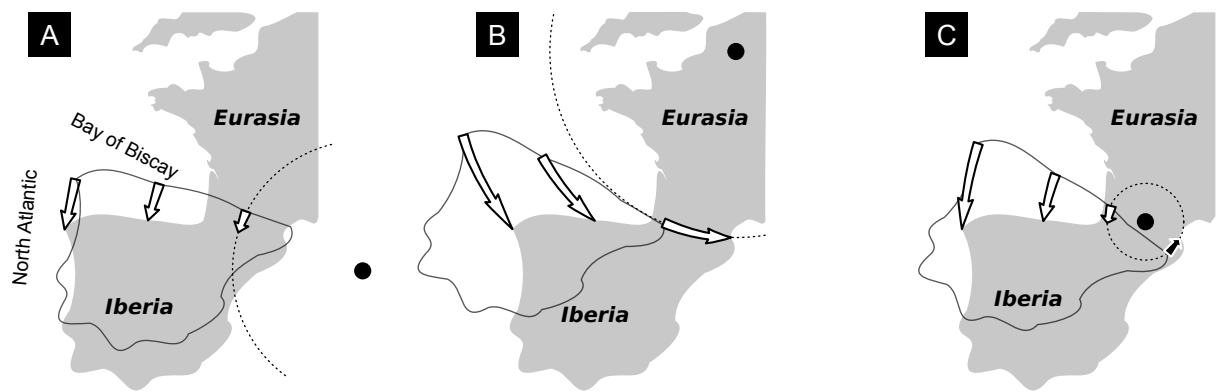
**Figure 1 (Two columns)**

Kinematic models proposed in the early 70's to explain the opening of the Bay of Biscay. The motion of Iberia with respect to fixed Eurasia is described by its rigid rotation about an Euler's pole located: (A) to the east of Iberia, (B) near Paris, (C) in the Pyrenean mountain range. Modified from Choukroune et al. (1973).
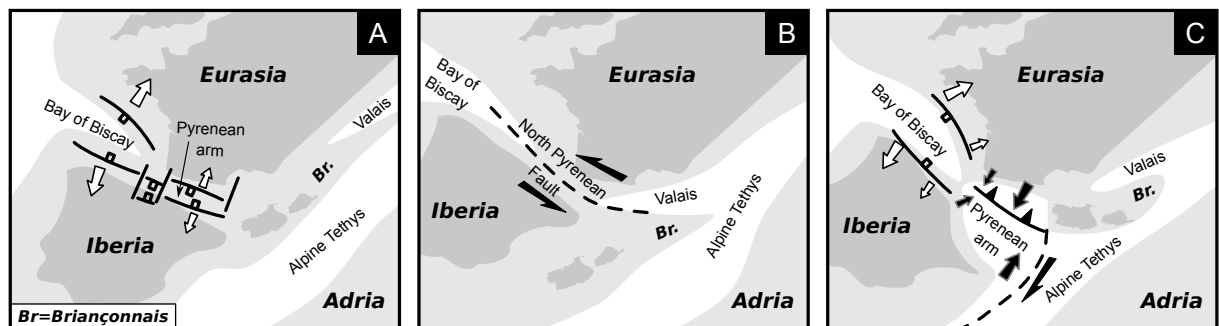
**Figure 2 (Two columns)**

Reconstructions of the Iberia-Eurasia margin and surrounding regions at the mid-Cretaceous time. (A) rift-perpendicular scenario, after Manatschal and Müntener (2009). (B) Strike-slip scenario, after Stampfli and Borel (2002). (C) Scissor scenario, after Advokaat et al., (2014).
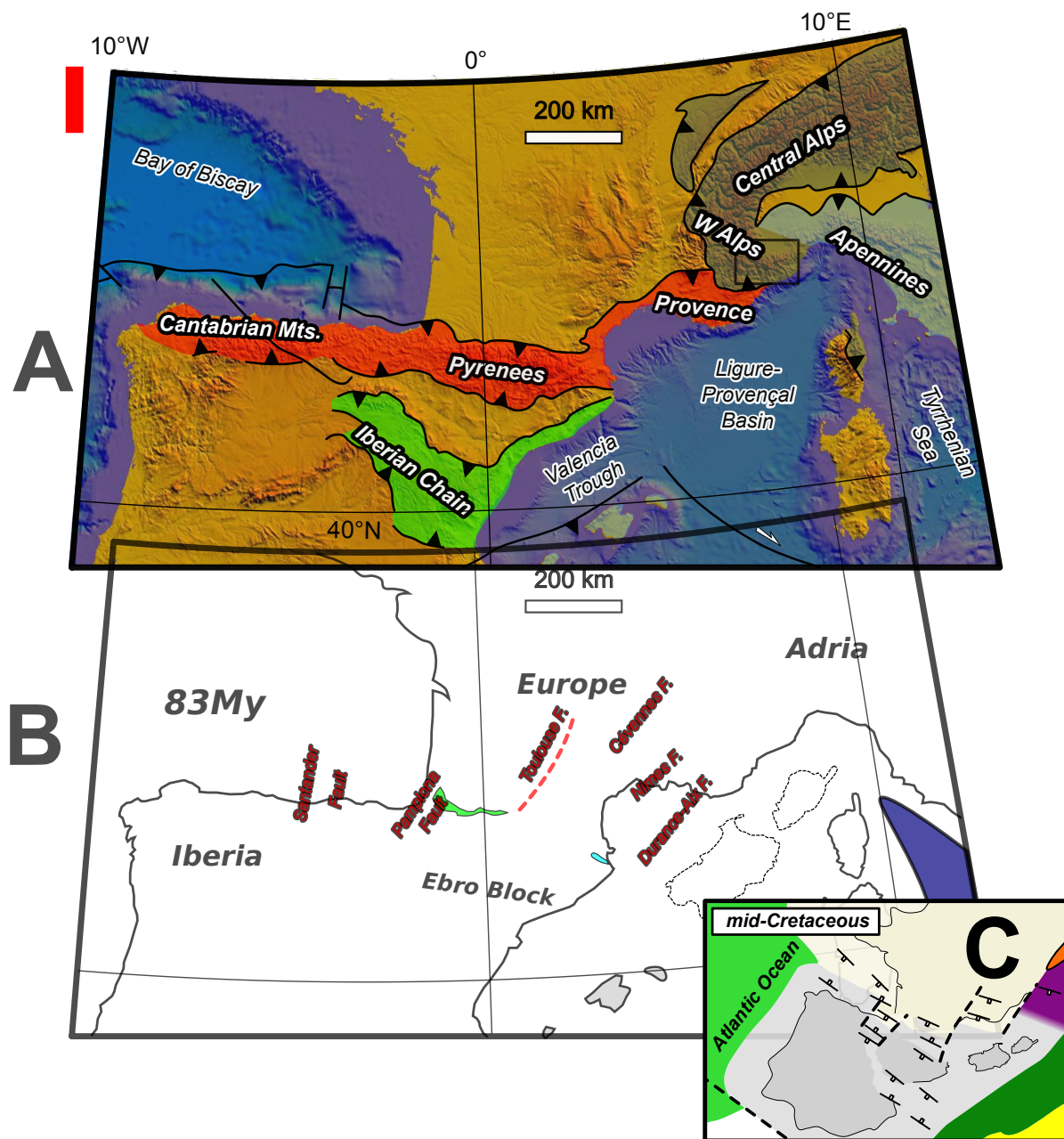
**Figure 3 (Two columns)**
Tectonic map of the westernmost Europe, with Late Cretaceous - Cenozoic belts and basins (A), and Mesozoic domains (B), with focus on the architecture of the Bay of Biscay – Pyrenean rift system. The distribution of Mesozoic domains is modified after Tugend et al. (2015) for the Bay of Biscay-Pyrenean area, and from Handy et al., (2010) for the Alps-Apennines area. The position of the Corsica-Sardinia block before the opening of the Ligure-Provencal basin is from Bache et al., (2010). (C) Reconstruction of the Iberia-Eurasia margin and surrounding domains in the mid-Cretaceous, modified from Manatschal and Müntener (2009)
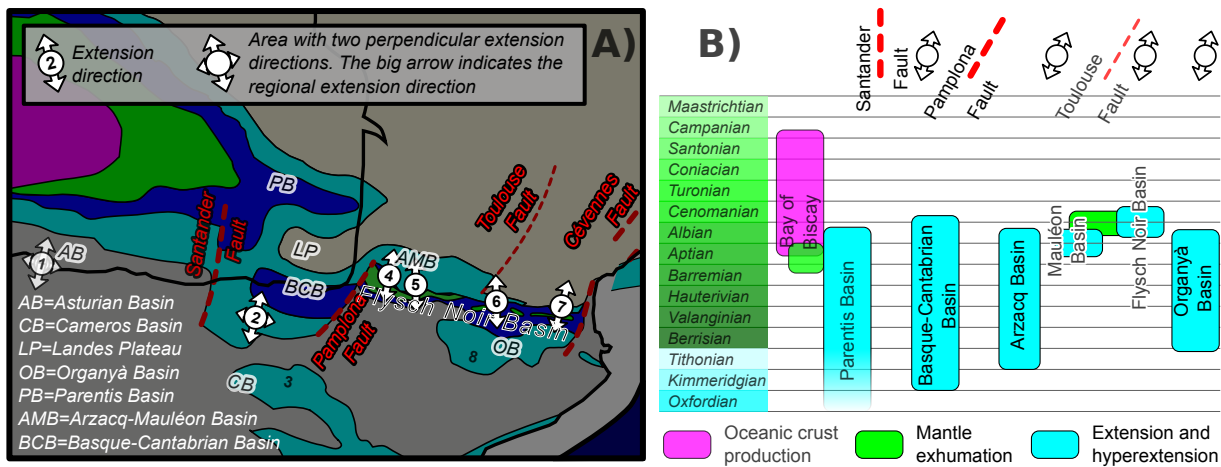
**Figure 4 (Two columns)**

Cretaceous extensional structures in the Pyrenean Arm. (A) Detail of the map in figure 3b in the Pyrenean area, with orientation of Cretaceous extension indicated. (B) Table illustrating the timing of major events and the direction of extensional structures in the different domains of the Pyrenean Arm and surrounding areas. References cited in the text and/or indicated in the figure are: Tugend et al. (2014) for the age of the oceanic crust in the Bay of Biscay. Thinon et al. (2003) and Roca et al. (2011) for the age of mantle exhumation in the Bay of Biscay. Ferrer et al. (2008) for the age of extension and hyperextension in the Parentis Basin. García-Mondéjar et al. (1986) and Rat (1988) for the age of extension in the Basque-Cantabrian Basin. Biteau et al. (2006) for the age of extension in the Arzacq Basin. Jammes et al. (2009), Lagabrielle et al. (2010), and Masini et al. (2014) for the age of hyperextension and mantle exhumation in the Mauléon Basin. Souquet et al. (1985) and Debroas (1990) for the age of extension and hyperextension in the Flysch Noir Basin. Dinarès-Turell and García-Senz (2000) and García-Senz (2002) for the age of extension in the Organyà basin. Granado et al. (In press) for the extension direction (meso-structural data) in the Asturian basin (indicated as site 1). Soto et al. (2008) and Oliva-Urcia et al. (2013) (AMS data), and  Tavani and Muñoz (2012) (meso- and macro-structural data) for the extension direction in the Basque-Cantabrian basin (indicated as site 2). Soto et al. (2008) and García-Lasanta et al. (2014) (AMS), and Mata et al. (2001) (meso-structural data) for the extension direction in the Cameros basin (indicated as site 3). Lagabrielle et al. (2010) for the extension direction (meso-structural data) in the Mauléon extensional detachment (indicated as site 4). Salardon et al. (2017) (meso-structural data) and Olivia-Urcia et al. (2010) (AMS) for the extension direction in the Mauléon basin (indicated as site 5). Passchier (1984) and de Saint Blanquat et al. (1986 and 1990) for the extension direction (meso-structural data) in the Saint Barthélémy massif extensional detachment (indicated as site 6). Vauchez et al. (2013) for the extension direction (meso-structural data) in the Agly massif extensional detachment (indicated as site 7). Gong et al. (2009) and Oliva-Urcia et al. (2011) (AMS data), and  Tavani et al. (2011) (meso- and macro-structural data) for the extension direction in the Organyà basin (indicated as site 8).
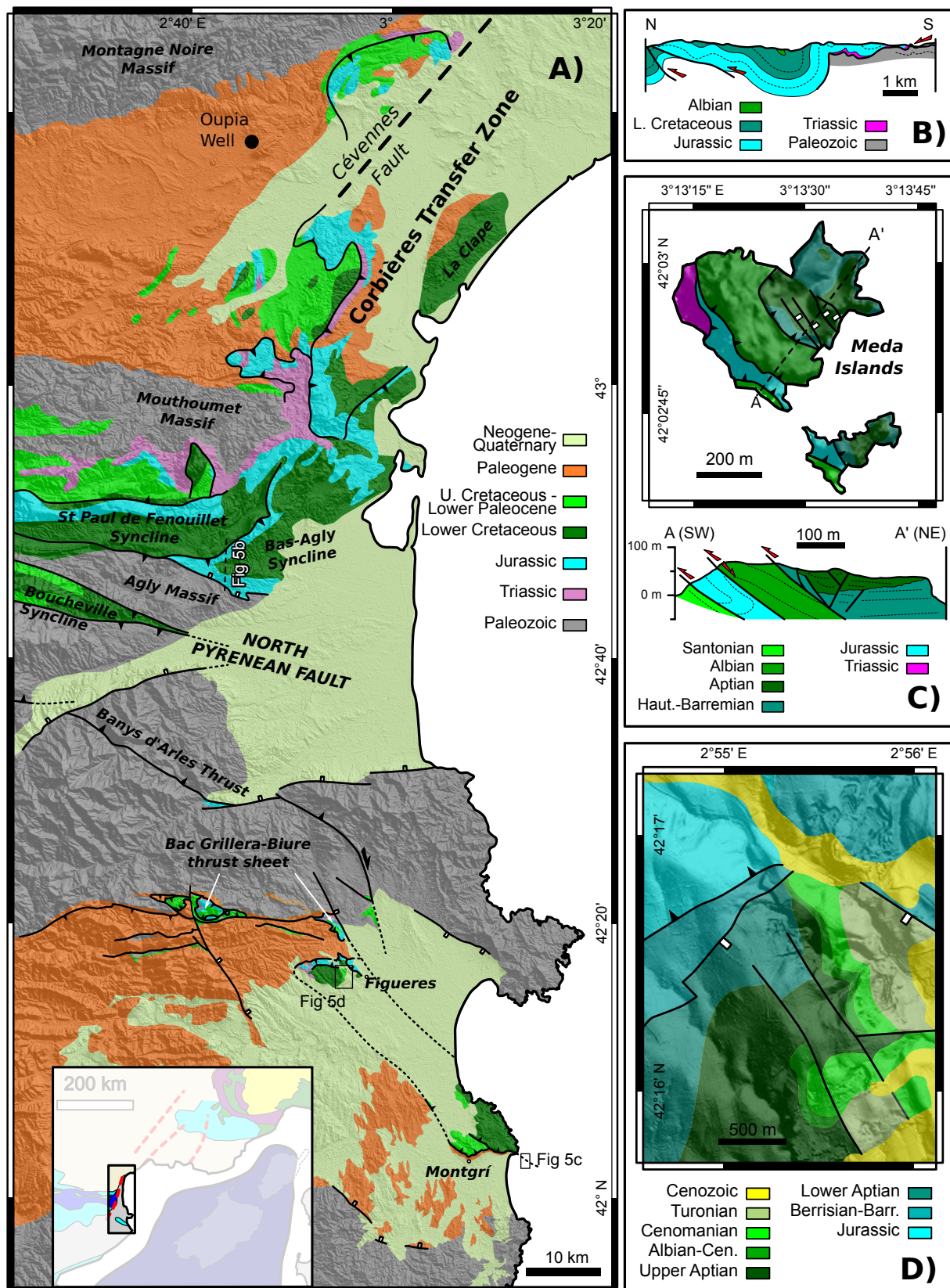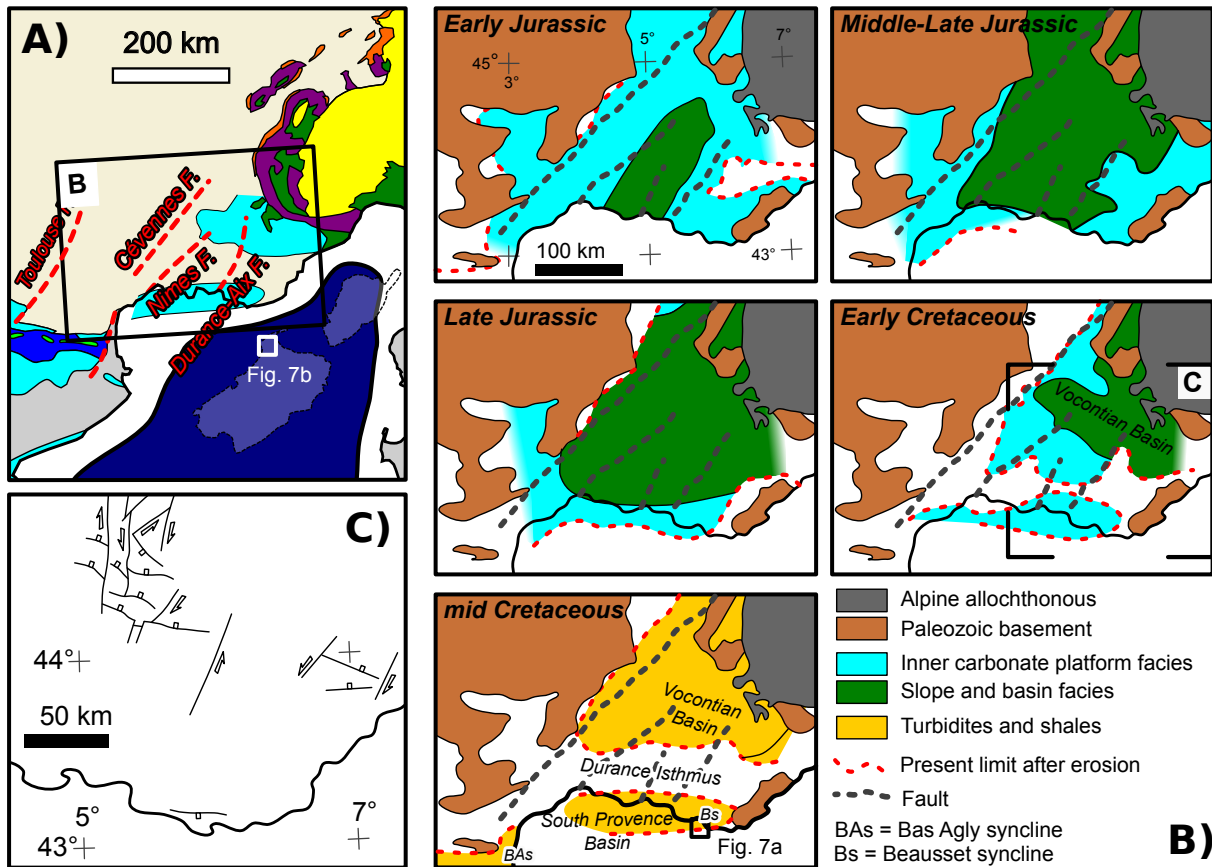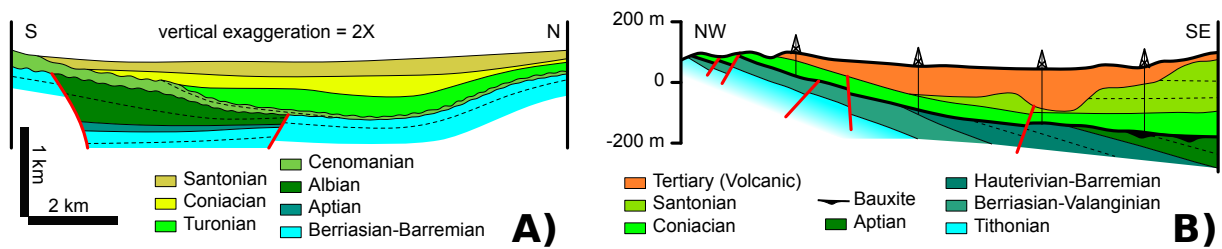
Figure 5
(A) Geological map of the eastern Pyrenees. (B) Cross section across the Bas Agly syncline (after Vauchez et al., 2013). (C) Cross section across the Meda Islands of the Montgrí area (after Mató et al., 1995b). (D) Geological map of the Figueres area.
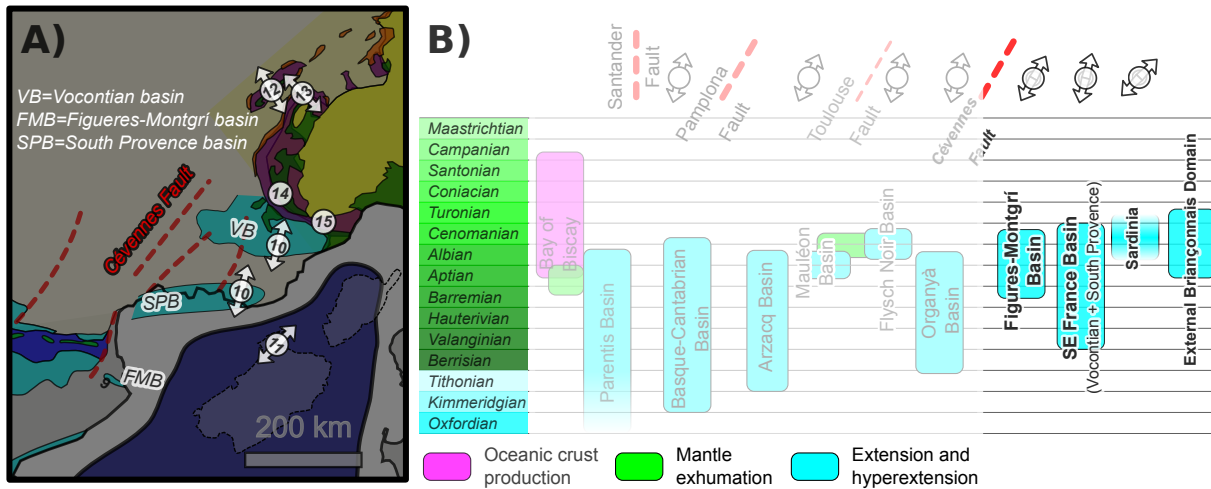
**Figure 6 (Two columns)**
(A) Detail of the map in figure 3b, showing the location of the Late Jurassic - Cretaceous extensional structures developed on the European margin of the Alpine Tethys, and presently exposed in the central and western Alps, in the Provence region of the Pyrenean System, and in Sardinia (B) Facies distribution in the SE Basin of France, from Triassic to mid-Cretaceous (after Curnelle and Dubois, 1986). (C) Simplified Early Cretaceous structural scheme of the SE Basin of France, with major faults indicated (after de Graciansky and Lemoine, 1988).

**Figure 7 (Two columns)**
(A) Schematic cross-section of the southern margin of the South Provence basin (after Philip et al.
(1987). (B) Cross-section of the Olmedo area in Sardinia (after Mameli et al. 2007).

**Figure 8 (Two columns)**

Cretaceous extensional structures in eastern Pyrenees and SE France basin. (A) Detail of the map in figure 3b in the area, with orientation of Cretaceous extension indicated. (B) Table illustrating the timing of major events and the direction of extensional structures in the different domains, with data from the Bay of Biscay - Pyrenean Arm in transparency. References cited in the text and/or indicated in the figure are: Saula et al. (1994) and Mató et al. (1995a, 1995b) for the age of extension in the Figueres-Montgrí basin. Guyonnet-Benaize et al. (2010) and Masse et al (2009) for the age of extension in the Vocontian and South Provence basins. Mameli et al. (2007) for the age of extension in the Olmedo area of Sardinia. Mató et al. (1995b) for the extension direction (syn-sedimentary faults orientation) in the Figueres-Montgrí (indicated as site 9). Guyonnet-Benaize et al. (2010), Lamarche et al. (2012), and Homberg et al. (2013) (meso-structures), and de Graciansky and Lemoine (1988) (major faults) for the extension direction in the Vocontian and South Provence basins (both indicated as site 10). Mameli et al. (2007) (orientation of an extensional fold) for the extension direction in the Olmedo area of Sardinia (indicated as site 11). Septfontaine (1995) for the age and direction (orientation of major fault) of extension in the Helvetic domain (indicated as site 12). Cardello and Mancktelow (2014) for the age and direction (meso- and macro-structures) of extension in the Helvetic domain (indicated as site 13), notice that this could be a gravitational-structure. Chaulieu (1992), Claudel et al. (1997), and Claudel and Dumont (1999) for the age of extension in the external Briançonnais Domain of the Western Alps (indicated as site 14).
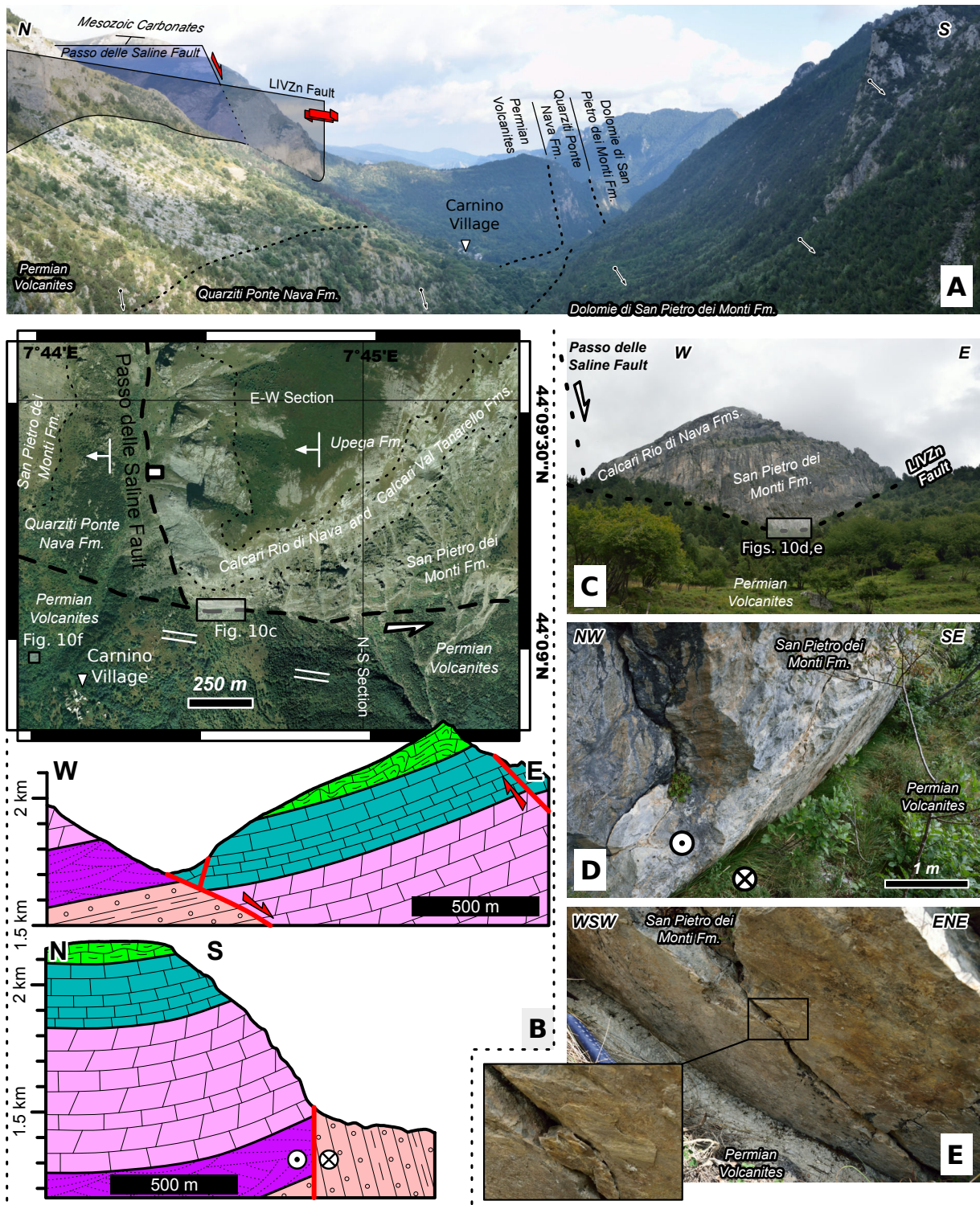
**Figure 9 (Single column)**
Geological maps of the Marguareis area.
(A) Map of the western Alps (modified
from d'Atri et al., 2015), with inset showing
the location of figure 9b. The arrows
indicate counter-clockwise rotations about
vertical axes (from Collombet et al., 2002).
(B) Map of the Marguareis area (from
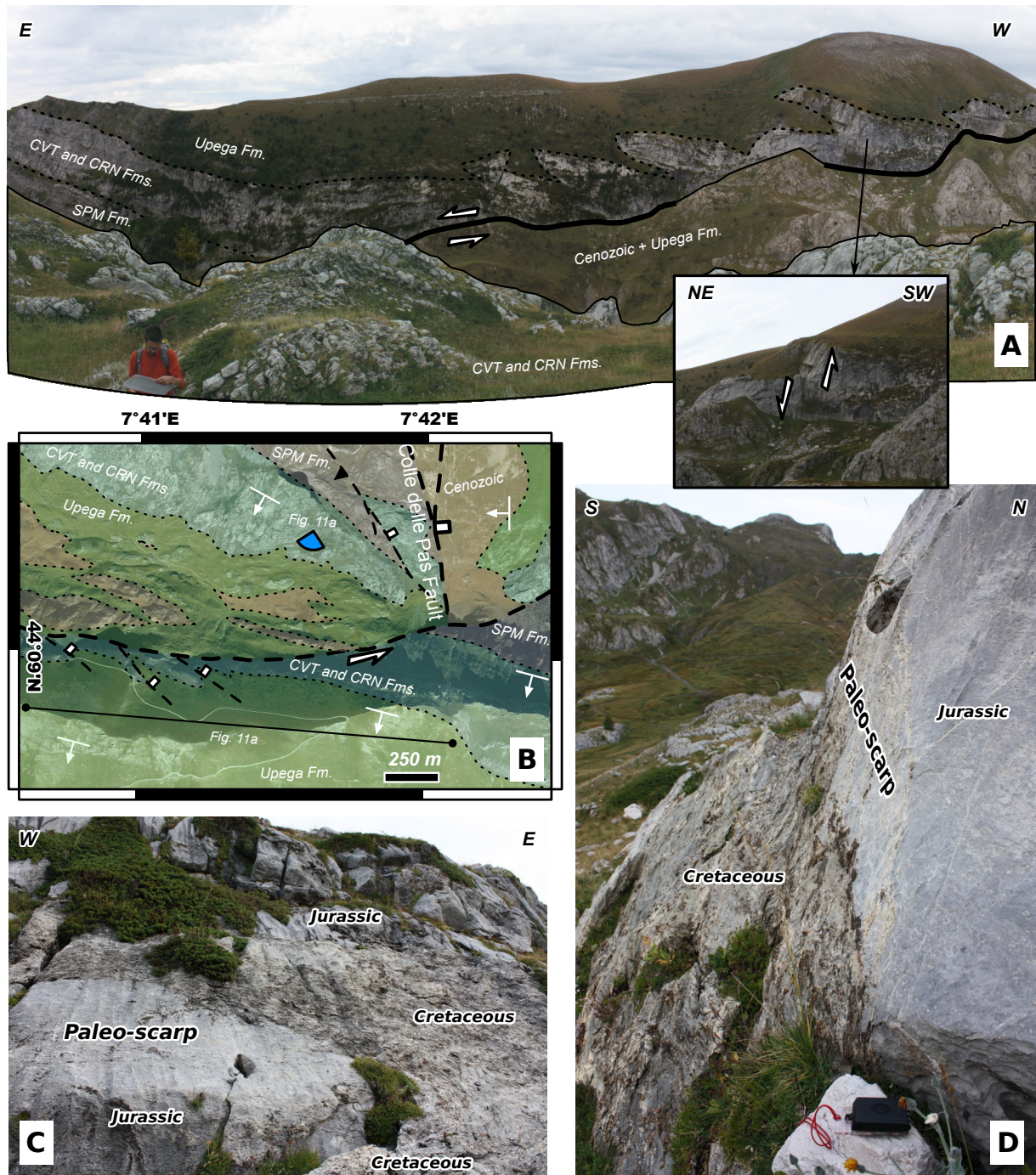Bertok et al., Submitted), with structural
scheme.

**Figure 10 (Two columns)**

Limone-Viozene northern (LIVZn) Fault in the eastern portion of the study area. (A) Panoramic view, from the west, of the LIVZn Fault, showing south-dipping Permo-Triassic rocks exposed in the southern block, and Triassic to Jurassic carbonates of the northern block, faulted by the Passo delle Saline Fault. (B) Orthophoto with structural scheme of the area and location of photographs and E-W and N-S oriented grological cross-sections (C) Panoramic view of the northern block of the LIVZn Fault: W-dipping Triassic and Jurassic carbonates are in the hanging-wall of the E-Dipping Passo delle Saline Fault, which abut onto the LIVZn Fault. (D) Principal displacement zone of the LIVZn Fault, with Permian Volcanites and Triassic dolostones in the southern and northern block, respectively. (E) Detail of the fault, showing calcite slicken-fibers indicating a left-lateral kinematics.
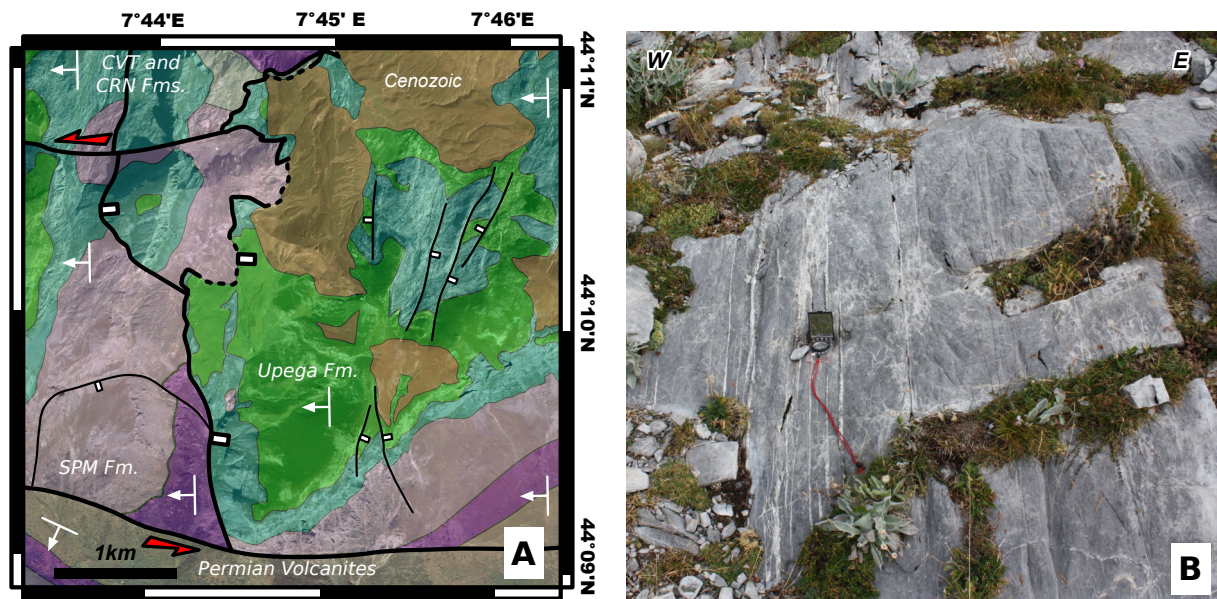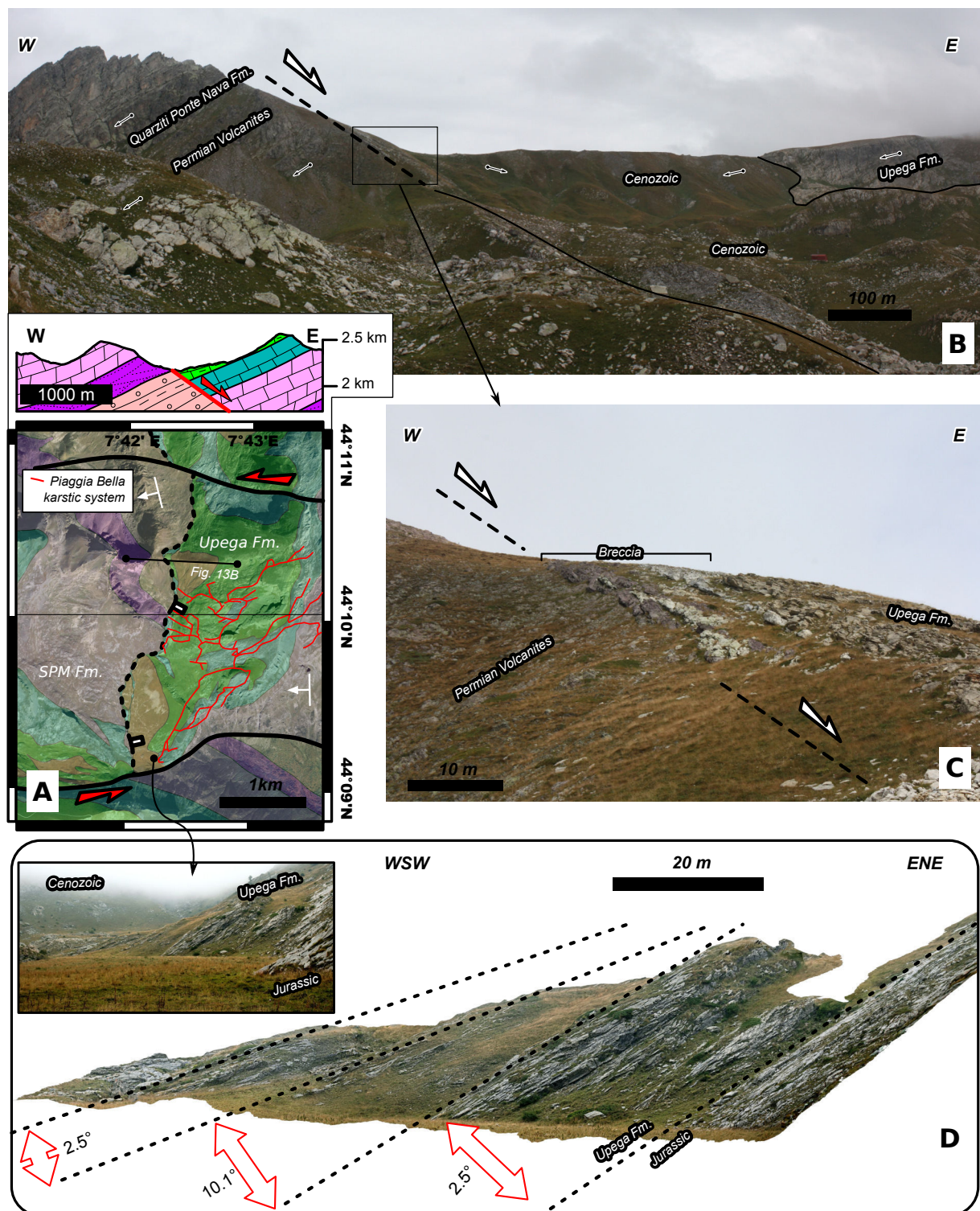
**Figure 11 (Two columns)**

Details of the LIVZn Fault in the western portion of the study area. (A) View from the north of the fault (for location of the photograph see Fig. 11b), with inset photograph showing a NW-SE striking normal fault in the southern block of the fault. (B) Orthophoto with structural scheme of the area and location of photographs. (C) and (D) E-W striking faults palaeoescarpment in Jurassic carbonates covered by patches of mid-Cretaceous sediments.

**Figure 12 (Two columns)**
(A) Orthophoto with structural scheme of the Passo delle Saline Fault area, showing hundreds of meters long N-S striking extensional faults. (B) N-S striking veins affecting Jurassic carbonates.
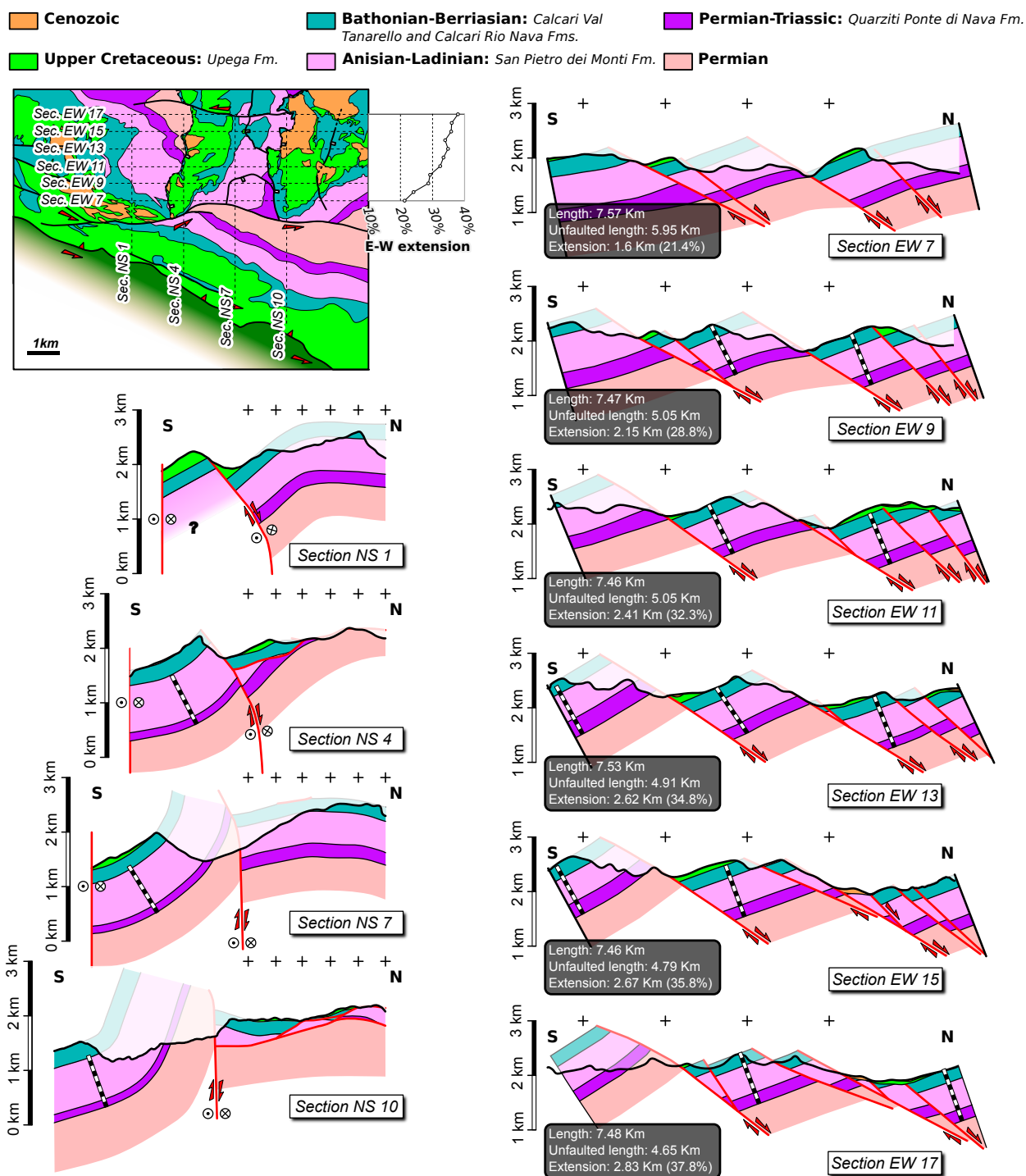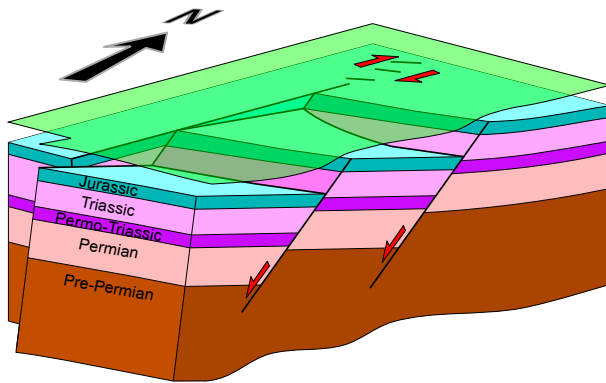
**Figure 13 (Two columns)**
(A) Orthophoto with structural scheme of the Colle del Pas Fault area and geological cross-section. (B) View from the south  of the fault, with W-dipping Permo-Triassic rock in the footwall and sub-horizontal to slightly W-dipping Upper Cretaceous and Cenozoic rocks in the hanging-wall. (C) Detail of the fault showing Permian volcanites underlying a 5-m thick breccia, which in turn is onlapped by Upper Cretaceous marls of the Upega Fm.. (D) Three-dimensional virtual outcrop model of the lower portion of the Upega Fm, built by means of multi-view photographs (see Tavani et al., 2016 details). The model is seen in orthographic view along a direction perpendicular to beddings, thus representing a distortion-free properly oriented cross-section of the outcrop, and shows a growth wedge of 15° in the lowermost portion of the Upega Fm.
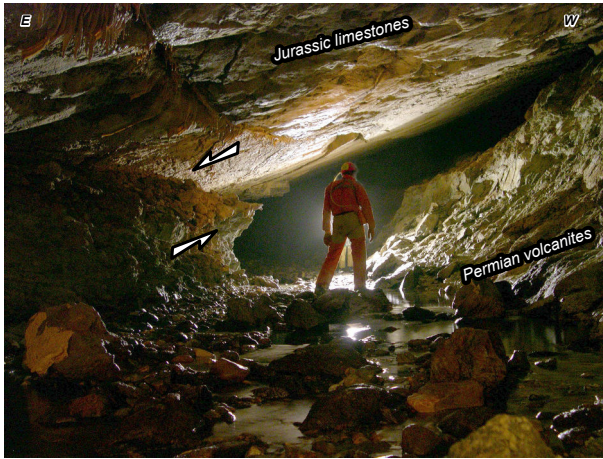
**Figure 14 (Single column)**
Photograph of Colle del Pas Fault plane as seen in the
Piaggia Bella Karstic system.

**Figure 15 (Two columns)**
E-W and N-S oriented cross-sections across the Marguareis extensional system. See text for details.

**Figure 16 (Single column)**
3D scheme illustrating the geometry of the
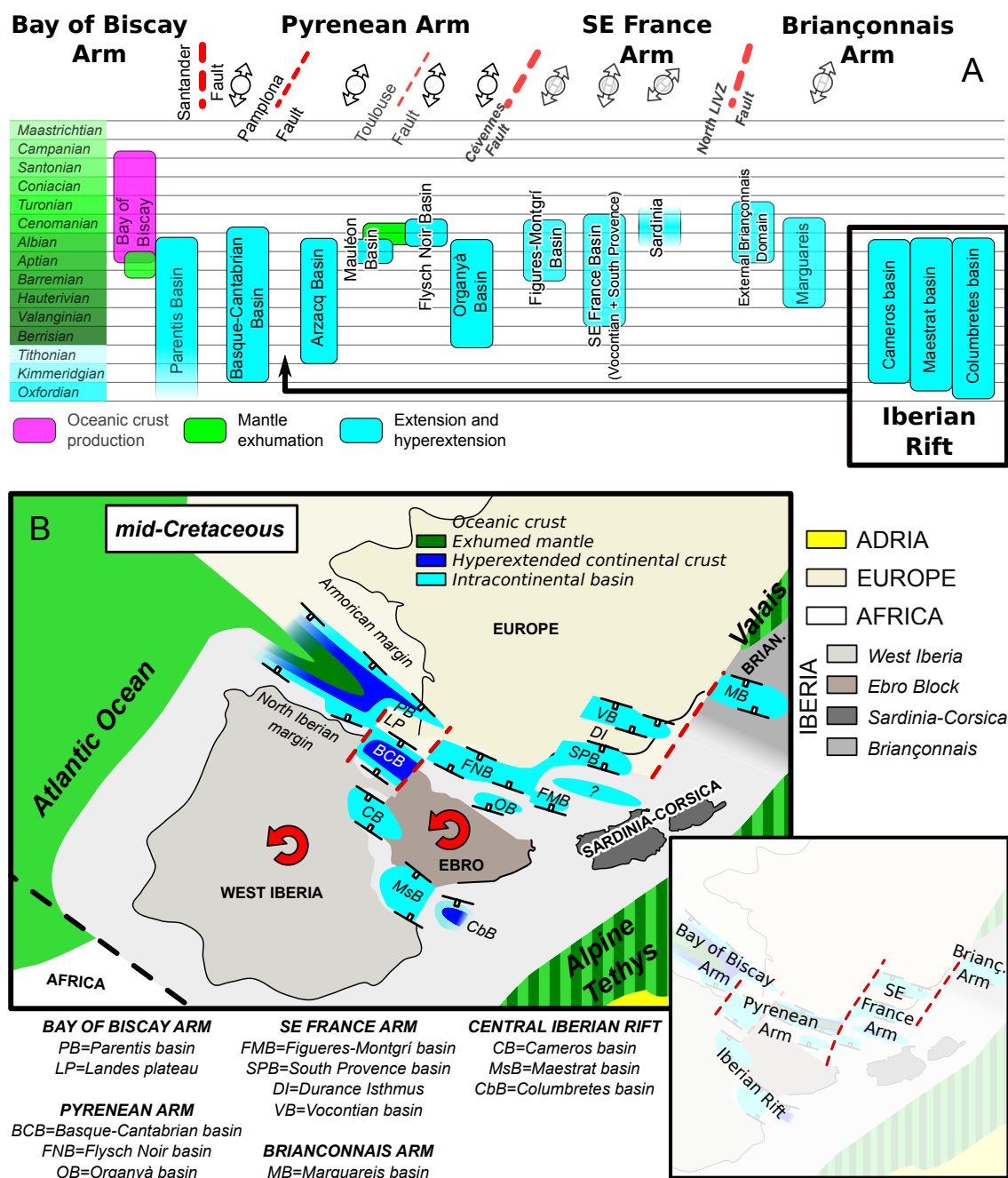Marguareis Extensional System at early Late
Cretaceous.

Figure 17
(A) Table illustrating the timing of major events and the direction of extensional structures in the different domains of the study area. (B) Reconstruction of the Iberia-Eurasia margin and surrounding areas in the mid-Cretaceous times, with major basins, transform faults, and crustal domains indicated.